Available online at www.sciencedirect.com

ScienceDirect

Geochimica et Cosmochimica Acta 221 (2018) 162–181

Geochimica et Cosmochimica Acta

www.elsevier.com/locate/gca

# Titanium isotopic compositions of rare presolar SiC grain types from the Murchison meteorite

Ann N. Nguyen [a,*], Larry R. Nittler [a], Conel M.O'D. Alexander [a], Peter Hoppe [b]

[a] Department of Terrestrial Magnetism, Carnegie Institution of Washington, Washington DC, USA
[b] Max Planck Institute for Chemistry, Mainz, Germany

Received 14 October 2016; accepted in revised form 19 February 2017; available online 27 February 2017

**Abstract**

We report the Ti isotopic compositions of 8 mainstream, 22 Y, 9 Z, and 26 AB presolar SiC grains from two SiC-rich residues of the Murchison CM2 meteorite together with Si, C and some Mg-Al isotopic data for the same grains. Mainstream, Y and Z grains are believed to originate in asymptotic giant branch (AGB) stars of varying metallicities, but the stellar sources of AB grains are poorly understood. We find that the $^{46,47,49}Ti/^{48}Ti$ ratios are correlated with $^{29}Si/^{28}Si$ for all of the grain types, indicating that these ratios are mainly dominated by Galactic chemical evolution (GCE). The mainstream, Y and Z grains all show enrichments in $^{50}Ti$ from neutron capture nucleosynthesis. However, AGB models predict smaller excesses in $^{50}Ti$ (and $^{49}Ti$) than are observed in these grains. For Z grains and especially for Y grains, the enhancement of $^{50}Ti$ is greater than the enhancement in $^{30}Si$, indicating that the $^{13}C$ neutron source produced a greater total fluence of neutrons than the $^{22}Ne$ source in the low metallicity parent AGB stars. The Z grains plot below the mainstream correlation lines at more $^{48}Ti$- and $^{28}Si$-rich compositions in plots of $^{46,47,49}Ti/^{48}Ti$ vs. $^{29}Si/^{28}Si$. On the other hand, the Y grains plot close to the mainstream correlation line. This could imply that the Ti isotopes evolved non-linearly at metallicities below ~1/3 solar. The AB grains in this study have Ti isotopic compositions that fall along correlation lines defined by the mainstream grains, suggesting origins in close to solar metallicity stars. However, these grains fall below the mainstream correlation lines in plots of $^{46,49,50}Ti/^{48}Ti$ vs. $^{29}Si/^{28}Si$ and do not show enhancements in $^{50}Ti$, indicating that their parent stars did not undergo significant *s*-process nucleosynthesis. These data support origins of AB grains in J-type C stars rather than born-again AGB stars that undergo *s*-process nucleosynthesis. AB grains that do not have $^{50}Ti$ excesses may provide the best measure of Si and Ti isotope GCE since their parent stars were less affected by *s*-process nucleosynthesis than the mainstream grains.


*Keywords:* Circumstellar grains; Galactic chemical evolution; Nucleosynthesis; Stars

## 1. INTRODUCTION

Presolar grains originating from the outflows and ejecta of evolved stars, such as asymptotic giant branch (AGB) stars, supernovae (SNe), and novae, are found in primitive meteorites, interplanetary dust particles (IDPs), and cometary dust returned by NASA's Stardust mission (Floss et al., 2013; Zinner, 2014). These grains are identified by their highly anomalous isotopic compositions relative to any solar system material. These isotopic compositions are the products of nucleosynthetic and mixing processes that occurred deep within their parent stars. The study of presolar grains in the laboratory has provided unprecedented insight into various astrophysical phenomena, such as Galactic chemical evolution (GCE), stellar nucleosynthesis and mixing, dust condensation in circumstellar environments, and dust processing in the interstellar medium (ISM) and the solar system.

* Corresponding author at: Jacobs, Astromaterials Research and Exploration Science Directorate, NASA Johnson Space Center, Houston, TX, USA.
*E-mail address:* lan-anh.n.nguyen@nasa.gov (A.N. Nguyen).

http://dx.doi.org/10.1016/j.gca.2017.02.026
0016-7037/

The first presolar grains to be isolated in the laboratory were the carbonaceous phases diamond, SiC, and graphite that have anomalous noble gas components (Bernatowicz et al., 1987; Lewis et al., 1987; Amari et al., 1990). Ion microprobe studies later identified highly anomalous isotopic compositions associated with several oxide and silicate phases, and $Si_3N_4$ (Hutcheon et al., 1994; Nittler et al., 1994, 1995, 1997; Messenger et al., 2003; Nguyen and Zinner, 2004). The analysis of individual roughly micron-sized grains was made possible by the development of the ion microprobe, and led to the identification of different sub-types of presolar grains having distinct stellar origins.

Presolar SiC grains are the best characterized presolar phase and have been the focus of many detailed presolar grain studies for multiple reasons. Unlike O-rich phases, all SiC grains in primitive meteorites have presolar origins and concentrated samples of SiC can be produced in the laboratory by acid dissolution techniques and gentle separation methods (Amari et al., 1994; Bernatowicz et al., 2003; Nittler and Alexander, 2003; Tizard et al., 2005). Moreover, presolar SiC grains can have diameters of several microns, with some unusually large grains exceeding 25 μm (Virag et al., 1992; Zinner et al., 2011). This makes it easier to analyze multiple isotopic systems in single grains. As such, the database of Si, C, and N isotopic compositions is very well established and several sub-types of presolar SiC have been classified based upon their Si, C, and N isotopic signatures (Hoppe et al., 1994; Zinner, 2014).

The most widely studied SiC grain sub-type, termed mainstream, makes up ~90% of all presolar SiC and has $^{12}C/^{13}C$ ratios in the range of 10–100 (terrestrial ~89). These grains are typically enriched in $^{29}Si$ and $^{30}Si$ by up to ~20% relative to the solar composition. They most likely condensed in low-mass C-rich AGB stars of approximately solar metallicity (Hoppe and Ott, 1997; Lugaro et al., 2003). Type Y grains have $^{12}C/^{13}C > 100$, are $^{30}Si$-rich and $^{29}Si$-poor relative to mainstream grains, and are believed to have originated in C-rich AGB stars of about one-half solar metallicity with masses up to 5 $M_\odot$ (Amari et al., 2001b). Z grains have $^{12}C/^{13}C$ between 10 and 100, similar to mainstream grains, are more $^{30}Si$-rich and $^{29}Si$-poor than Y grains, and likely condensed in AGB stars of about one-third solar metallicity (Alexander, 1993; Hoppe et al., 1997; Zinner et al., 2007). SiC X grains have compositions (e.g., enrichments in $^{28}Si$ and $^{15}N$ and a wide range of $^{12}C/^{13}C$ ratios) pointing to Type II supernova (SN) sources (Nittler et al., 1996). The latter three grain types each make up ~1–2% of all presolar SiC. Z grains are predominantly found among submicrometer-sized grains. Type C SiC grains are extremely rare (~0.1%) and likely have SN origins as well (Hoppe et al., 2012; Xu et al., 2015; Liu et al., 2016). However, while X grains are enriched in $^{28}Si$, C grains show excesses in $^{29}Si$ and $^{30}Si$ (Amari et al., 1999; Hoppe et al., 2010, 2012). A few grains with marked excesses in $^{13}C$ and $^{15}N$ could have nova origins (Amari et al., 2001a), though additional isotopic analyses of some putative nova grains indicate SN origins instead (Nittler and Hoppe, 2005; Liu et al., 2016). Type A and B grains are more abundant (~5%), but their parent stellar sources are ambiguous. These grains are enriched in $^{13}C$ with $^{12}C/^{13}C < 10$, show both enrichments and depletions in $^{15}N$, and have Si isotopic distributions similar to mainstream grains. The N and Si isotopic compositions of AB grains are distinct from the putative nova grains. Proposed stellar sources include born-again AGB stars or J-type carbon stars (Alexander, 1993; Hoppe et al., 1994; Amari et al., 2001c). Excess $^{32}S$ in three AB grains support born-again AGB stars as the source of some of these grains (Fujiya et al., 2013). One AB grain shows enhancements in *r*-process and *p*-process isotopes of Mo and Ru, suggesting material transfer from a Type II SN in a binary system (Savina et al., 2003, 2007), though the *p*-process likely occurs in multiple astrophysical settings. Recent multi-element isotopic analyses of some $^{15}N$-rich AB grains also suggest possible origins in Type II SNe (Nittler et al., 2016). In all cases, the isotopic compositions of the AB grains are not well understood within the context of existing nucleosynthesis models.

The isotopic compositions of many trace elements, including Mg-Al, S, Ti, Fe, Ni, Mo, Zr, Ru, and Ba, have been measured in presolar SiC grains owing to their relatively high concentrations (Amari et al., 1995). Of the tens of thousands of presolar SiC identified, there are only ~250 published analyses of Ti isotopic ratios, with most being mainstream and X grains (Hoppe et al., 1994; Nittler et al., 1996; Alexander and Nittler, 1999; Amari et al., 2001b, 2001c; Hoppe and Besmehn, 2002; Nittler and Hoppe, 2005; Gyngard et al., 2006; Huss and Smith, 2007; Zinner et al., 2007; Lin et al., 2010; Fujiya et al., 2013). X grains typically have excesses in $^{49}Ti$ attributed to the decay of $^{49}V$ (half-life = 330 d) and n-capture nucleosynthesis, and excesses in $^{44}Ca$ from the decay of $^{44}Ti$ (half-life = 60 yr), which is only produced in SN explosions (Amari et al., 1992; Hoppe et al., 1996, 2000; Nittler et al., 1996; Hoppe and Besmehn, 2002; Lin et al., 2010). In AGB stars, the C and N isotopic compositions are affected by core and shell H- and He-burning, whereas the Si and Ti isotopes are affected by slow neutron capture (*s*-process) nucleosynthesis. Most of the Si and Ti isotopic ratios of SiC grains from AGB stars are more strongly affected by the initial stellar compositions, reflecting GCE (Hoppe et al., 1994; Gallino et al., 1997, 1998; Alexander and Nittler, 1999; Amari et al., 2001b). However, the effects of *s*-process nucleosynthesis on Ti isotopes are stronger in lower-metallicity stars, making Ti data for the Y and Z grains highly desirable to test models of both GCE and AGB nucleosynthesis. For example, the Ti isotopic compositions of some Z grains confirmed a low-metallicity origin for the grains but some discrepancies with *s*-process nucleosynthesis models were found (Zinner et al., 2007). The number of grains in this study was limited, however.

Although the Ti isotope systematics of mainstream and X-type SiC grains are reasonably well understood, there are far fewer data for the rare Y, Z, and AB types. We report here C, Si, and Ti isotopic data for 8 mainstream, 22 Y, 9 Z, and 26 AB SiC grains from the Murchison meteorite. We also discuss the Mg-Al isotopic data for 5 AB grains that were previously reported by Zinner et al. (2007). These

data will improve our understanding of the Galactic and stellar processes that affect Ti isotopic ratios in AGB stars of varying metallicities and our understanding of the stellar origins of the enigmatic AB grains.

## 2. EXPERIMENTAL

### 2.1. Samples

We chose for analysis rare SiC grains that came from two SiC residues of the Murchison CM2 chondrite. The Muri11B sample was prepared at the MPI for Chemistry in Mainz (Besmehn and Hoppe, 2003) using the separation technique employed in Amari et al. (1994). The grain size distribution of this fraction was ~0.2–5 μm. The MUR52 sample was prepared at Carnegie by a different chemical dissolution procedure that used CsF rather than HF to digest silicate material (Nittler and Alexander, 2003). This sample had grain sizes of ~0.5–4 μm prior to the isotopic analyses. For both residues, the grains were deposited onto gold foils from suspension in isopropanol-water solutions.

### 2.2. Isotopic analyses

The SiC grains analyzed in this study were first analyzed for their Si and C isotopic compositions by an automated mapping system in the Carnegie Cameca IMS-6f ion microprobe (Nittler and Alexander, 2003). In this method, ion images are used to identify dispersed particles. A 1–2 μm $Cs^+$ primary ion beam is then deflected and focused onto each particle in turn and the isotopes are measured in peak-jumping mode. A total of 1,150 SiC grains were measured with reasonable errors (<~15 for $^{12}C/^{13}C$, <~50‰ for $\delta^{29}Si$, and <~115‰ for $\delta^{30}Si$; see supplementary Table ES1) from the Muri11B sample; data for a few of these grains have been reported previously (Nittler and Hoppe, 2005; Zinner et al., 2007). A total of 1,551 grains (1,550 SiC and one $Si_3N_4$) were analyzed in the MUR52 sample; one highly $^{13}C$-enriched grain from this survey was reported by Liu et al. (2016).

The Ti isotopic measurements were performed on select grains with the Carnegie Cameca NanoSIMS 50L equipped with 7 electron multipliers. The grains were chosen based on their belonging to rare presolar SiC groups and on there being sufficient material remaining following the Si and C isotopic analyses. All grains were less than a micron in size (~600 nm on average) after the initial isotopic analyses. Compared to previous NanoSIMS measurements of Ti in presolar SiC (e.g., Zinner et al., 2007), the larger magnet on the NanoSIMS 50L allows for simultaneous collection of all 5 Ti isotopes without requiring peak-jumping (Stadermann et al., 2005; Zinner et al., 2007). Positive secondary ions of $^{46}Ti$, $^{47}Ti$, $^{48}Ti$, $^{49}Ti$, $^{50}Ti$, $^{28}Si$ and $^{52}Cr$ were thus measured concurrently using an $O^-$ primary ion beam. Synthetic titanium carbide grains served as isotopic standards. SiC grains were identified from $^{28}Si^+$ and $^{48}Ti^+$ raster images, and the isotopic measurements of individual grains were performed in "grain mode" where the primary beam was rastered over an area around the grain no larger than $3 \times 3\ \mu m^2$ with a scanning frame of $64 \times 64$ pixels$^2$. Each region was measured for 130–1400 cycles, with an integration time of 0.541 s/cycle, and the data were subdivided into blocks with 10 cycles/block. The $^{48}Ti$ count rate was monitored during the analysis to look for possible internal TiC grains. Chromium-52 was measured to correct for the isobaric interference from $^{50}Cr$, assuming a normal $^{50}Cr/^{52}Cr$ ratio. Corrections for possible Ca and V interferences were not made because previous studies indicated that they are very small (<3‰) (Zinner et al., 2007).

## 3. RESULTS

The complete Si- and C-isotopic data set for the SiC and $Si_3N_4$ grains identified in the Muri11B and MUR52 samples through automated measurements is reported in supplementary Table ES1. Fig. 1 shows the $^{30}Si/^{28}Si$ ratio plotted versus the $^{12}C/^{13}C$ ratio for the 2,700 grains automatically analyzed for Si and C isotopes. Open symbols indicate grains for which we obtained Ti-isotopic data. We express Si and Ti isotopic ratios in this paper in δ-notation, or deviations from solar in parts per thousand (‰). For Si, $\delta^i Si/^{28}Si = [(^iSi/^{28}Si)_{grain}/(^iSi/^{28}Si)_{solar} - 1] \times 1000$. Similarly for Ti, $\delta^i Ti/^{48}Ti = [(^iTi/^{48}Ti)_{grain}/(^iTi/^{48}Ti)_{solar} - 1] \times 1000$. Several grains with highly unusual compositions have been reported previously (e.g., grains with low $^{12}C/^{13}C$ ratios, Nittler and Hoppe, 2005; Liu et al., 2016). The $^{12}C$- and $^{30}Si$-rich grain M52B-505-1 has a close-to-solar $\delta^{29}Si$ value of $23 \pm 12$‰. This grain was not analyzed for Ti, but a NanoSIMS measurement revealed it to have isotopically light N ($^{14}N/^{15}N \approx 3800$). The possible stellar source of this grain is discussed further in Section 4.3.

The Ti isotopic compositions were determined for 8 mainstream, 22 Y, 9 Z, and 26 AB SiC grains. The Si and C isotopic ratios for these grains and inferred $^{26}Al/^{27}Al$ ratios for 5 of the grains are given in Table 1 and the Si isotopic compositions are shown in Fig. 2. The Ti isotopic compositions of the SiC grains from this study are given in Table 2 and shown in Fig. 3. Also shown in these figures are literature data for the SiC grains for which the Ti isotopes were measured. The correlation lines shown in Figs. 2 and 3 were calculated by Zinner et al. (2007) for mainstream SiC grains.

The Si isotopic ratios of the grains in the current study fall within the ranges previously observed for the respective SiC grain populations. Y grains are typically enriched in $^{30}Si$ relative to mainstream SiC grains and thus fall to the right of the mainstream correlation line. However, 6 of the Y grains in this study lie to the left of the mainstream correlation line. The Z grains in our study exhibit Si isotopic ratios that are typical for this population. These grains are generally depleted in $^{29}Si$ and have larger $^{30}Si$ enrichments than Y grains. The AB grains have Si isotopic ratios that fall in the range observed for mainstream SiC grains.

The Ti isotopic compositions of the SiC grains in this study generally fall in the ranges of compositions previously observed (Fig. 3). In both the $\delta^{47}Ti$ vs. $\delta^{46}Ti$ and $\delta^{49}Ti$ vs. $\delta^{46}Ti$ plots, our grain data lie close to the mainstream correlation lines defined by the literature data. The Y and AB

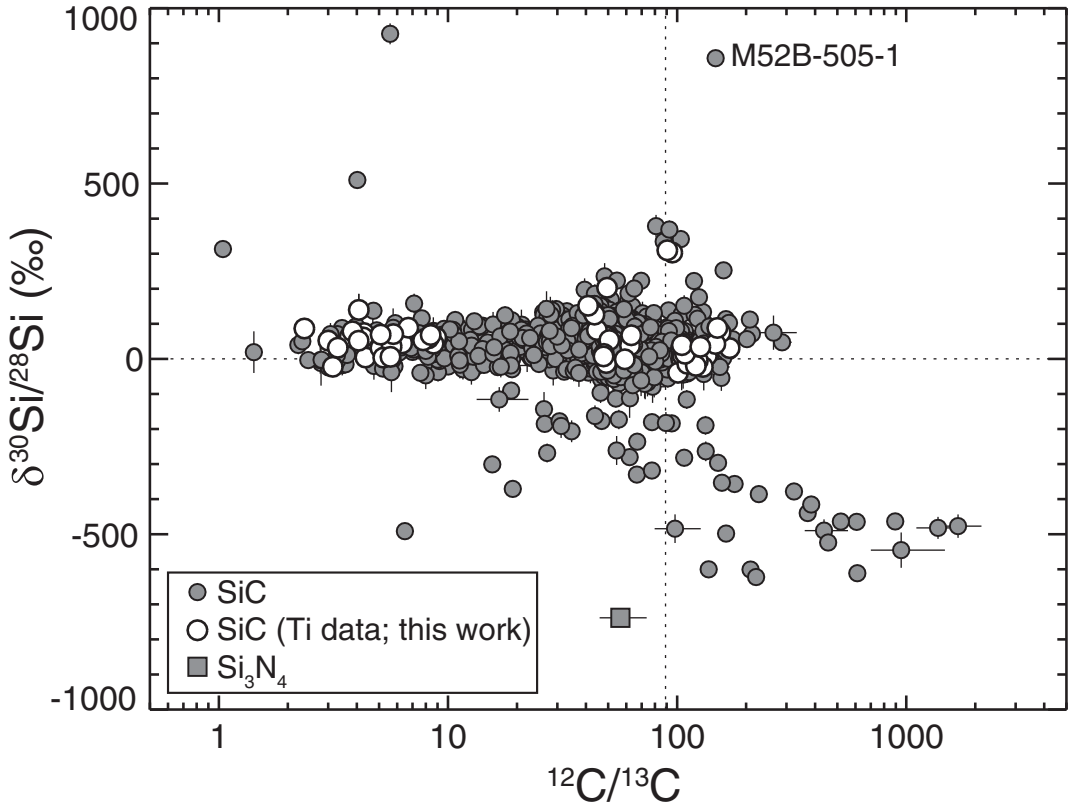


Fig. 1. $\delta^{30}Si/^{28}Si$ values and $^{12}C/^{13}C$ ratios of presolar SiC grains and one $Si_3N_4$ grain identified by automated Si- and C-isotopic measurements (Nittler and Alexander, 2003). Open symbols indicate grains for which Ti isotopic ratios were determined in this study. Dashed lines indicate solar isotopic compositions.

grains have compositions that are within the range for mainstream grains. The Z grains also plot along the mainstream correlation lines, but have more negative $\delta^{46}Ti$ compositions. In the $\delta^{50}Ti$ vs. $\delta^{46}Ti$ plot, the AB grains closely follow the mainstream correlation line and cover approximately the same range as mainstream SiC grains, but have on average smaller $^{50}Ti$ enhancements than the other grain types. The mainstream, Y and Z grains show progressively larger $^{50}Ti$ enrichments relative to the correlation lines.

For mainstream grains, it was previously observed that the Ti and Si isotopic systems are strongly correlated (Hoppe et al., 1994). In Fig. 4, the Ti isotopic compositions of the grains in our study and from previous studies are plotted against $\delta^{29}Si$. Most of the mainstream grains from this study also show correlated Ti and Si isotopic ratios. Exceptions are grains M52B-596-3, M52B-723-1, and M52B-750-1, which plot well below the mainstream lines for $\delta^{46}Ti$, $\delta^{49}Ti$, and $\delta^{50}Ti$ vs. $\delta^{29}Si$. As seen in previous studies, the Y grains generally overlap the distribution for mainstream grains and show positive correlations in their Ti and Si isotopic ratios. However, some of the grains have greater $^{50}Ti$ enrichments and the slope for the fit to the Y grain data in the $\delta^{50}Ti$ vs. $\delta^{29}Si$ plot is steeper compared to the mainstream grains. The Z grains show positive correlations for $\delta^{46}Ti$, $\delta^{47}Ti$, and $\delta^{49}Ti$ vs. $\delta^{29}Si$ that have similar (in the case of $\delta^{47}Ti$ vs. $\delta^{29}Si$) and steeper (for $\delta^{46}Ti$ and $\delta^{49}Ti$ vs. $\delta^{29}Si$) slopes than the mainstream correlation lines and are shifted to lower intercepts. The distribution of $\delta^{50}Ti$ values for the Z grains is very similar to Y grains, but there does not appear to be a correlation with $\delta^{29}Si$. The AB grains from this study plot in the range observed previously for AB and mainstream grains in the $\delta^{46}Ti$, $\delta^{47}Ti$, and $\delta^{49}Ti$ vs. $\delta^{29}Si$ plots, though the AB grains tend to lie below the mainstream correlation line. The AB grains also have lower $\delta^{50}Ti$ values than the mainstream grains.

The $^{48}Ti$ and $^{28}Si$ count rates were monitored during the analysis of each grain. For most grains, the Ti count rate remained constant throughout the measurements, suggesting that the Ti was uniformly distributed (i.e., in solid solution), while in other grains large variations in Ti count rates during the measurements indicate the presence of internal TiC subgrains. Fig. 5 shows the change in the $^{28}Si$ and $^{48}Ti$ counts during the analysis of two grains that likely had internal subgrains. While the $^{28}Si$ counts steadily drop as the grains are sputtered away, there are clear peaks in the $^{48}Ti$ counts. Statistics were too low in cases like these to determine Ti-isotopic compositions for individual TiC subgrains. We found that two (25%) of the mainstream grains, 8 (36%) Y grains, 4 (44%) Z grains, and 5 (19%) of the AB grains showed peaks in their $^{48}Ti$ count rates during their analyses and likely had internal TiC subgrains. Thus, approximately the same proportions of Y and Z grains have internal TiC subgrains, whereas mainstream and AB grains appear to have fewer internal TiC subgrains. We did not

Table 1
Silicon, C, and inferred Al isotopic compositions of presolar SiC grains in this study.

| Grain | Type | $^{12}C/^{13}C$ | $\delta^{29}Si/^{28}Si$ | $\delta^{30}Si/^{28}Si$ | $^{26}Al/^{27}Al$ ($\times10^{-3}$) |
|---|---|---|---|---|---|
| M52-25-1 | Mainstream | 62.3 ± 1.0 | 47 ± 12 | 38 ± 21 | |
| M52B-596-3 | Mainstream | 40.9 ± 0.9 | 193 ± 14 | 151 ± 19 | |
| M52B-703-1 | Mainstream | 59.1 ± 0.9 | −31 ± 7 | −1 ± 10 | |
| M52B-723-1 | Mainstream | 27.1 ± 0.3 | 138 ± 7 | 118 ± 10 | |
| M52B-724-1 | Mainstream | 47.7 ± 0.5 | −45 ± 7 | 7 ± 9 | |
| M52B-747-1 | Mainstream | 47.9 ± 0.5 | −59 ± 7 | 14 ± 9 | |
| M52B-750-1 | Mainstream | 62.1 ± 0.6 | 50 ± 8 | 60 ± 11 | |
| M52B-764-1 | Mainstream | 63.1 ± 0.6 | 58 ± 5 | 67 ± 8 | |
| M52B-8-15 | AB | 5.6 ± 0.1 | 13 ± 19 | 6 ± 20 | |
| M52B-99-2 | AB | 5.1 ± 0.1 | 122 ± 26 | 69 ± 33 | |
| M52B-104-2 | AB | 6.3 ± 0.1 | 0 ± 13 | 44 ± 19 | |
| M52B-122-2 | AB | 7.9 ± 0.2 | 14 ± 17 | 57 ± 19 | |
| M52B-123-10 | AB | 6.7 ± 0.1 | 27 ± 18 | 89 ± 26 | |
| M52B-131-1 | AB | 4.3 ± 0.05 | 9 ± 10 | 61 ± 17 | |
| M52B-131-3 | AB | 3.1 ± 0.1 | 16 ± 14 | −23 ± 29 | |
| M52B-133-10 | AB | 8.7 ± 0.2 | 80 ± 11 | 43 ± 12 | |
| M52B-150-1 | AB | 8.2 ± 0.1 | 76 ± 10 | 59 ± 16 | |
| M52B-163-1 | AB | 2.4 ± 0.02 | 57 ± 11 | 87 ± 13 | |
| M52B-164-1 | AB | 5.1 ± 0.04 | 52 ± 7 | 31 ± 9 | |
| M52B-224-1 | AB | 7.8 ± 0.5 | 9 ± 20 | 53 ± 38 | |
| M52B-224-11 | AB | 8.4 ± 0.2 | 67 ± 10 | 68 ± 18 | |
| M52B-227-1 | AB | 3.3 ± 0.1 | 37 ± 11 | 32 ± 14 | |
| M52B-356-2 | AB | 5.7 ± 0.05 | 26 ± 8 | 35 ± 11 | |
| M52B-371-1 | AB | 5.8 ± 0.1 | 80 ± 9 | 71 ± 11 | |
| M52B-513-12 | AB | 3.4 ± 0.03 | 12 ± 11 | 30 ± 16 | |
| M52B-513-8 | AB | 4.1 ± 0.1 | 159 ± 27 | 140 ± 46 | |
| M52B-520-2 | AB | 3.8 ± 0.1 | 16 ± 15 | 79 ± 17 | |
| M52B-703-17 | AB | 4.1 ± 0.1 | 63 ± 10 | 52 ± 13 | |
| M52B-729-12 | AB | 5.2 ± 0.1 | 1 ± 10 | 4 ± 12 | |
| Muri11B-80-2 | AB | 8.9 ± 0.3 | 50 ± 9 | 61 ± 17 | 2.53 ± 0.277 |
| Muri11B-160-1 | AB | 3.7 ± 0.04 | 107 ± 9 | 63 ± 17 | 2.26 ± 0.317 |
| Muri11B-275-1 | AB | 3.0 ± 0.03 | 4 ± 9 | 52 ± 17 | 2.04 ± 0.836 |
| Muri11B-287-3 | AB | 4.4 ± 0.1 | −22 ± 9 | 4 ± 17 | 5.83 ± 0.252 |
| Muri11B-428-1 | AB | 4.3 ± 0.1 | 28 ± 12 | 74 ± 18 | 18.4 ± 0.806 |
| M52B-3-1 | Y | 110.7 ± 3.6 | −30 ± 12 | −14 ± 13 | |
| M52-38-1 | Y | 129.7 ± 7.2 | 76 ± 17 | 134 ± 22 | |
| M52B-96-6 | Y | 104.9 ± 4.4 | −20 ± 13 | 39 ± 16 | |
| M52B-96-7 | Y | 126.2 ± 9.5 | −30 ± 23 | 34 ± 24 | |
| M52B-129-2 | Y | 129.6 ± 12.0 | −27 ± 24 | −23 ± 37 | |
| M52B-129-6 | Y | 104.1 ± 3.1 | −22 ± 14 | 1 ± 30 | |
| M52B-133-5 | Y | 103.8 ± 3.1 | 5 ± 10 | 28 ± 13 | |
| M52-152-8 | Y | 175.0 ± 24.9 | −13 ± 25 | 56 ± 48 | |
| M52B-158-3 | Y | 100.8 ± 4.3 | −33 ± 15 | −40 ± 23 | |
| M52-172-1 | Y | 126.4 ± 2.5 | 8 ± 11 | 52 ± 17 | |
| M52-180-5 | Y | 134.8 ± 7.7 | −20 ± 14 | 9 ± 21 | |
| M52B-196-9 | Y | 105.5 ± 7.9 | −14 ± 19 | 10 ± 25 | |
| M52B-205-1 | Y | 107.5 ± 3.0 | −16 ± 12 | 26 ± 14 | |
| M52-213-1 | Y | 119.4 ± 4.4 | 8 ± 14 | −3 ± 22 | |
| M52B-227-8 | Y | 123.1 ± 7.2 | −9 ± 27 | −5 ± 32 | |
| M52B-253-1 | Y | 114.7 ± 4.8 | −39 ± 11 | 23 ± 15 | |
| M52B-253-2 | Y | 169.5 ± 8.1 | −19 ± 19 | 31 ± 22 | |
| M52B-385-4 | Y | 154.7 ± 3.5 | 42 ± 12 | 75 ± 13 | |
| M52B-567-4 | Y | 146.9 ± 8.1 | −14 ± 9 | 43 ± 11 | |
| M52B-702-15 | Y | 149.8 ± 6.2 | 83 ± 11 | 88 ± 13 | |
| M52B-703-3 | Y | 120.7 ± 5.4 | −22 ± 16 | −20 ± 22 | |
| M52B-723-8 | Y | 108.2 ± 1.7 | −6 ± 11 | 15 ± 13 | |
| M52-11-7 | Z | 42.7 ± 0.8 | −97 ± 15 | 137 ± 19 | |
| M52-37-3 | Z | 49.5 ± 5.4 | −99 ± 29 | 203 ± 37 | |
| M52B-151-1 | Z | 49.1 ± 1.1 | −67 ± 12 | 63 ± 17 | |
| M52B-164-3 | Z | 95.3 ± 5.6 | −73 ± 23 | 303 ± 24 | |
| M52B-166-2 | Z | 49.0 ± 0.9 | −71 ± 10 | −12 ± 13 | |

Table 1 (*continued*)

| Grain | Type | $^{12}C/^{13}C$ | $\delta^{29}Si/^{28}Si$ | $\delta^{30}Si/^{28}Si$ | $^{26}Al/^{27}Al$ ($\times10^{-3}$) |
|---|---|---|---|---|---|
| M52B-166-7 | Z | 44.7 ± 0.9 | −58 ± 12 | 82 ± 16 | |
| M52B-597-10 | Z | 43.6 ± 1.1 | −4 ± 12 | 126 ± 13 | |
| M52B-702-8 | Z | 90.6 ± 4.2 | −148 ± 20 | 310 ± 23 | |
| M52B-729-5 | Z | 50.6 ± 1.0 | −72 ± 8 | 54 ± 11 | |

*Note* – Isotopic ratio errors are 1σ. Ratios given as δ-values are in permil (‰). $^{26}Al/^{27}Al$ ratios were measured with the NanoSIMS 50 ion microprobe at the MPI for Chemistry in Mainz and were previously reported in Zinner et al. (2007).

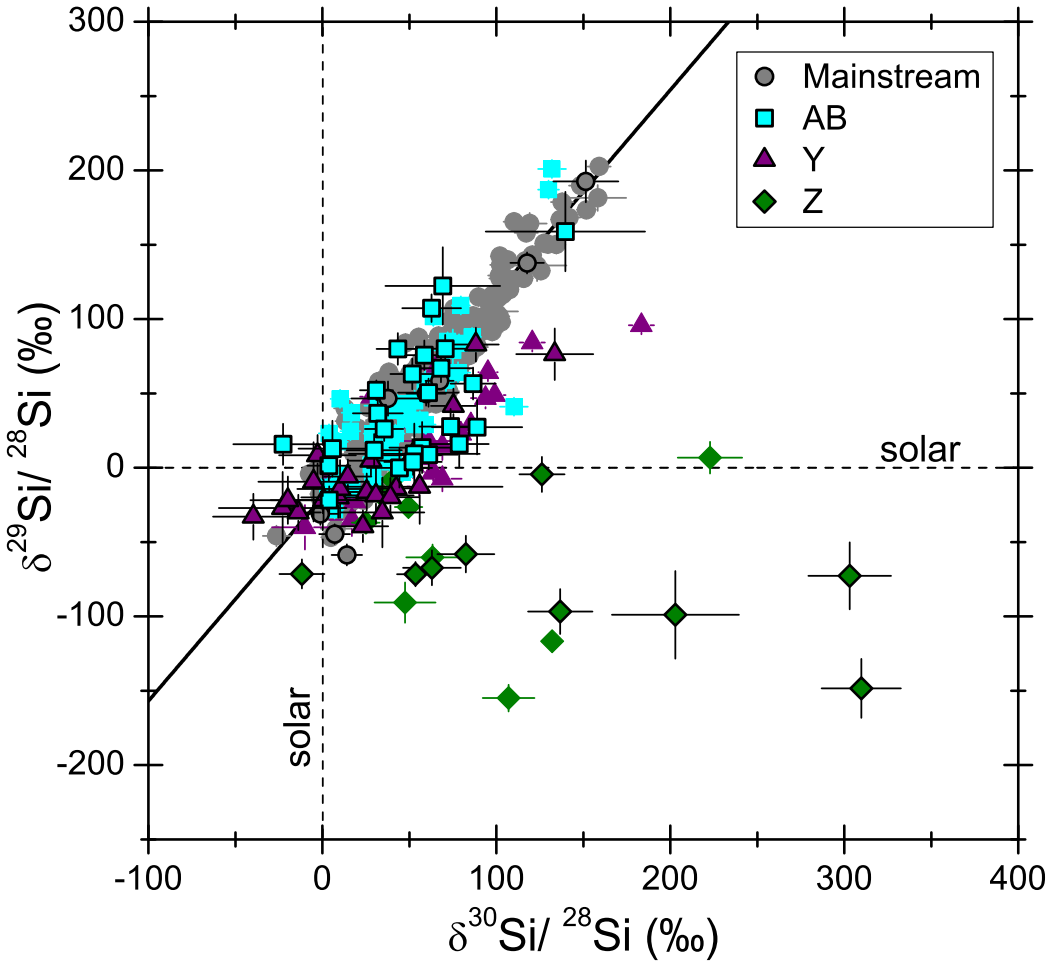


Fig. 2. Silicon isotopic compositions of presolar SiC grains analyzed in this study for Ti (symbols outlined in black). Also shown are presolar SiC grains from the literature for which Ti isotopes were also analyzed (Virag et al., 1992; Hoppe et al., 1994; Alexander and Nittler, 1999; Amari et al., 2001b, 2001c; Nittler and Hoppe, 2005; Huss and Smith, 2007; Zinner et al., 2007). The dashed lines indicate solar isotopic ratios and the solid line denotes the mainstream correlation line as determined by Zinner et al. (2007).

measure a SiC standard with known Ti contents, and thus cannot estimate absolute Ti concentrations in the grains. However, the average $^{48}Ti^+/^{28}Si^+$ ratios measured in the NanoSIMS for the Y and Z grains were similar (~0.03). Mainstream and AB grains had lower average Ti concentrations with $^{48}Ti^+/^{28}Si^+ = 0.02$.

## 4. DISCUSSION

Presolar SiC grains have been found to have isotopic signatures consistent with condensation in a variety of stellar sources. The atmospheres of these sources must have been C-rich (C > O) in order for SiC grains to have condensed (Lodders and Fegley, 1997). The vast majority of the grains have origins in C-rich AGB stars, but other sources include SNe and possibly novae. The source(s) of AB grains is more uncertain, with J-type stars and born-again AGB stars being the most likely candidates (Alexander, 1993; Amari et al., 2001c). In this section, we will first describe the relevant nucleosynthetic processes of AGB stars that affect the isotopic compositions of AGB-derived SiC grains. The isotopic compositions of the mainstream, Y, and Z grains will

Table 2
Titanium isotopic compositions of presolar SiC grains in this study.

| Grain | Type | $\delta^{46}Ti/^{48}Ti$ | $\delta^{47}Ti/^{48}Ti$ | $\delta^{49}Ti/^{48}Ti$ | $\delta^{50}Ti/^{48}Ti$ |
|---|---|---|---|---|---|
| M52-25-1 | Mainstream | −28 ± 7 | −24 ± 7 | 29 ± 9 | 190 ± 20 |
| M52B-596-3 | Mainstream | 4 ± 20 | 28 ± 24 | −32 ± 21 | 87 ± 32 |
| M52B-703-1 | Mainstream | 8 ± 6 | −5 ± 6 | 11 ± 8 | 189 ± 32 |
| M52B-723-1 | Mainstream | −65 ± 27 | −8 ± 26 | −2 ± 30 | 13 ± 32 |
| M52B-724-1 | Mainstream | −41 ± 4 | −39 ± 5 | −17 ± 6 | 142 ± 6 |
| M52B-747-1 | Mainstream | −1 ± 7 | 4 ± 7 | −12 ± 9 | 8 ± 22 |
| M52B-750-1 | Mainstream | −89 ± 17 | −106 ± 21 | −92 ± 22 | −52 ± 52 |
| M52B-764-1 | Mainstream | 17 ± 4 | 7 ± 4 | 107 ± 5 | 184 ± 10 |
| M52B-8-15 | AB | −46 ± 38 | −88 ± 39 | −49 ± 56 | 3 ± 71 |
| M52B-99-2 | AB | 43 ± 7 | 20 ± 6 | 39 ± 8 | 11 ± 9 |
| M52B-104-2 | AB | −70 ± 5 | −47 ± 5 | 3 ± 5 | 2 ± 5 |
| M52B-122-2 | AB | 1 ± 14 | −8 ± 13 | 62 ± 14 | 112 ± 16 |
| M52B-123-10 | AB | −78 ± 5 | −28 ± 6 | −13 ± 7 | 2 ± 6 |
| M52B-131-1 | AB | 5 ± 18 | −5 ± 18 | 9 ± 18 | 51 ± 25 |
| M52B-131-3 | AB | −49 ± 7 | −26 ± 9 | −23 ± 10 | −76 ± 9 |
| M52B-133-10 | AB | 49 ± 8 | 28 ± 8 | 72 ± 11 | 86 ± 12 |
| M52B-150-1 | AB | −27 ± 15 | 5 ± 15 | 29 ± 19 | 35 ± 92 |
| M52B-163-1 | AB | −23 ± 37 | −46 ± 40 | 57 ± 41 | 92 ± 49 |
| M52B-164-1 | AB | 36 ± 5 | 0 ± 5 | 101 ± 6 | 26 ± 7 |
| M52B-224-1 | AB | 11 ± 15 | 24 ± 19 | 70 ± 21 | 99 ± 29 |
| M52B-224-11 | AB | 31 ± 7 | 2 ± 6 | 104 ± 8 | 181 ± 9 |
| M52B-227-1 | AB | −17 ± 12 | 7 ± 12 | 28 ± 15 | 39 ± 16 |
| M52B-356-2 | AB | −38 ± 8 | −16 ± 8 | 6 ± 9 | −96 ± 9 |
| M52B-371-1 | AB | 9 ± 28 | −66 ± 29 | 74 ± 33 | 95 ± 29 |
| M52B-513-12 | AB | −67 ± 7 | −32 ± 7 | −38 ± 8 | −118 ± 9 |
| M52B-513-8 | AB | 78 ± 16 | 22 ± 16 | 163 ± 21 | 218 ± 22 |
| M52B-520-2 | AB | 32 ± 70 | 1 ± 34 | −34 ± 56 | 39 ± 43 |
| M52B-703-17 | AB | −13 ± 6 | −20 ± 7 | 14 ± 8 | −39 ± 8 |
| M52B-729-12 | AB | −33 ± 6 | −19 ± 7 | 9 ± 8 | 143 ± 9 |
| Muri11B-80-2 | AB | −26 ± 10 | −32 ± 11 | −11 ± 13 | −3 ± 26 |
| Muri11B-160-1 | AB | 58 ± 5 | 31 ± 5 | 79 ± 6 | 114 ± 7 |
| Muri11B-275-1 | AB | 34 ± 13 | 19 ± 16 | 101 ± 18 | 130 ± 32 |
| Muri11B-287-3 | AB | −24 ± 4 | −16 ± 4 | 1 ± 4 | −39 ± 7 |
| Muri11B-428-1 | AB | 49 ± 9 | 51 ± 10 | 137 ± 12 | 179 ± 14 |
| M52B-3-1 | Y | 24 ± 10 | −6 ± 10 | 50 ± 10 | 304 ± 11 |
| M52-38-1 [a] | Y | 10 ± 28 | 24 ± 30 | 50 ± 35 | 249 ± 749 |
| M52B-96-6 | Y | −61 ± 40 | −42 ± 42 | 18 ± 61 | −144 ± 50 |
| M52B-96-7 | Y | −103 ± 34 | −93 ± 32 | −113 ± 43 | 17 ± 48 |
| M52B-129-2 | Y | −32 ± 40 | −126 ± 61 | −89 ± 53 | −63 ± 57 |
| M52B-129-6 | Y | 16 ± 18 | 2 ± 14 | 88 ± 16 | 175 ± 20 |
| M52B-133-5 | Y | 4 ± 10 | −16 ± 11 | 32 ± 14 | 246 ± 16 |
| M52-152-8 | Y | −28 ± 16 | −4 ± 19 | 83 ± 20 | 235 ± 22 |
| M52B-158-3 | Y | −29 ± 32 | −52 ± 33 | 10 ± 38 | 53 ± 38 |
| M52-172-1 | Y | −13 ± 7 | −28 ± 8 | 19 ± 10 | 309 ± 11 |
| M52-180-5 | Y | −21 ± 10 | −14 ± 11 | 41 ± 13 | 129 ± 13 |
| M52B-196-9 | Y | 34 ± 15 | 19 ± 15 | 86 ± 20 | 223 ± 23 |
| M52B-205-1 | Y | 8 ± 20 | 32 ± 18 | 71 ± 21 | 323 ± 29 |
| M52-213-1 | Y | 43 ± 21 | −3 ± 20 | 38 ± 22 | 162 ± 32 |
| M52B-227-8 | Y | −12 ± 46 | −57 ± 38 | 47 ± 46 | 112 ± 55 |
| M52B-253-1 | Y | −1 ± 12 | 0 ± 14 | 51 ± 14 | 230 ± 14 |
| M52B-253-2 | Y | −79 ± 82 | −51 ± 59 | −68 ± 59 | 65 ± 69 |
| M52B-385-4 | Y | 39 ± 6 | 4 ± 6 | 74 ± 7 | 510 ± 9 |
| M52B-567-4 | Y | −37 ± 9 | −12 ± 10 | 40 ± 12 | 166 ± 14 |
| M52B-702-15 | Y | 74 ± 11 | 1 ± 11 | 101 ± 12 | 275 ± 13 |
| M52B-703-3 | Y | 10 ± 16 | 33 ± 20 | 31 ± 20 | 254 ± 26 |
| M52B-723-8 | Y | 25 ± 12 | −26 ± 14 | 92 ± 15 | 347 ± 21 |
| M52-11-7 | Z | −170 ± 20 | −65 ± 20 | −146 ± 24 | 40 ± 30 |
| M52-37-3 | Z | −178 ± 11 | −97 ± 20 | −162 ± 16 | −26 ± 17 |
| M52B-151-1 | Z | −103 ± 21 | −49 ± 29 | −41 ± 26 | 53 ± 37 |
| M52B-164-3 | Z | −199 ± 22 | −127 ± 26 | −147 ± 28 | 231 ± 32 |
| M52B-166-2 | Z | 6 ± 26 | −33 ± 30 | 6 ± 40 | 62 ± 32 |

Table 2 (*continued*)

| Grain | Type | $\delta^{46}Ti/^{48}Ti$ | $\delta^{47}Ti/^{48}Ti$ | $\delta^{49}Ti/^{48}Ti$ | $\delta^{50}Ti/^{48}Ti$ |
|---|---|---|---|---|---|
| M52B-166-7 | Z | −167 ± 12 | −45 ± 14 | −101 ± 18 | 7 ± 17 |
| M52B-597-10 | Z | −219 ± 10 | −109 ± 10 | −177 ± 12 | 151 ± 16 |
| M52B-702-8 | Z | −275 ± 15 | −135 ± 16 | −202 ± 21 | 346 ± 25 |
| M52B-729-5 | Z | −163 ± 14 | −161 ± 14 | −181 ± 18 | −146 ± 34 |

*Note* – Isotopic ratio errors are 1σ. Ratios are given as δ-values in permil (‰).
[a] The large $\delta^{50}Ti$ uncertainties for these grains are due to large $^{50}Cr$ interferences.

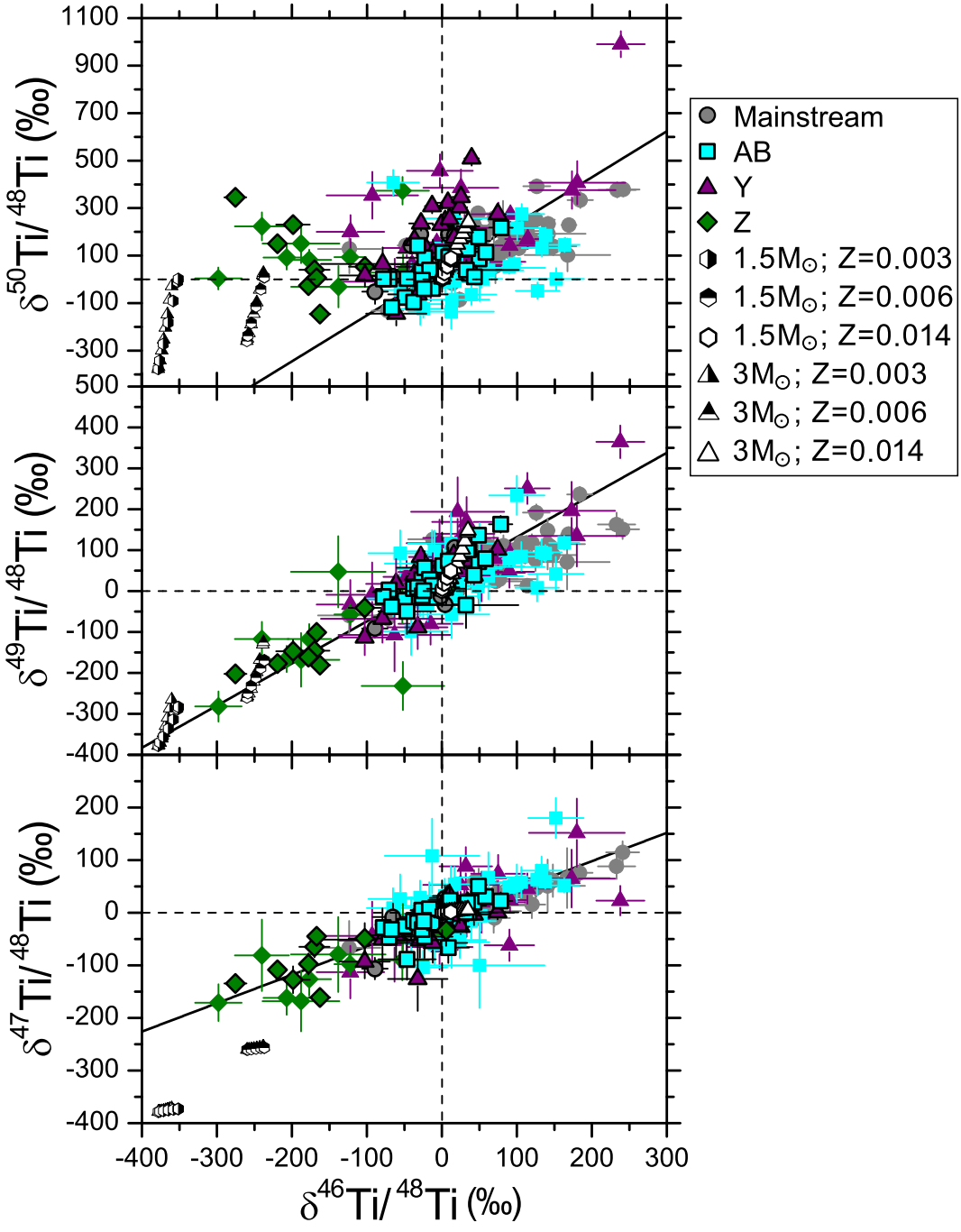


Fig. 3. Titanium isotopic compositions of presolar SiC grains from this study and from the literature given in permil (‰). Symbols and references are the same as in Fig. 2. Also shown are AGB nucleosynthesis models of Cristallo et al. (2011) for two different stellar masses and three different metallicities. The dashed lines indicate solar isotopic ratios and the solid lines denote mainstream correlation lines as determined by Zinner et al. (2007).

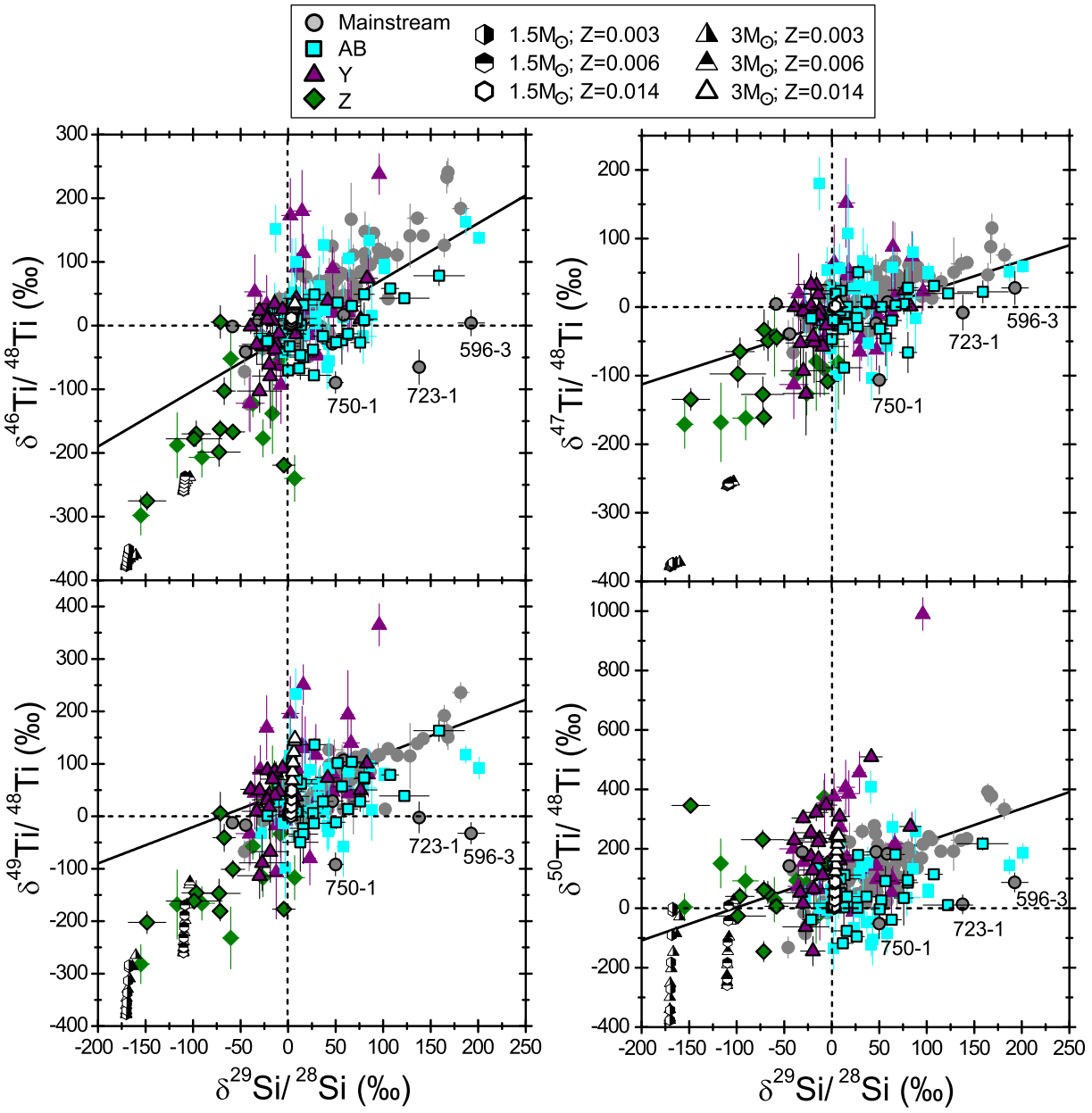


Fig. 4. Titanium isotopic compositions of presolar SiC grains compared to their $\delta^{29}Si/^{28}Si$ values. Symbols and references are the same as in Fig. 2. Also shown are AGB nucleosynthesis models of Cristallo et al. (2011) for two different stellar masses and three different metallicities. The three labeled grains fall below the mainstream correlation line and are discussed in Section 4.1.1. All ratios are given in delta notation in permil (‰). The dashed lines represent solar isotopic compositions and the solid lines are fits to the mainstream SiC grains.

be discussed in the context of astrophysical models. The possible stellar sources and isotopic compositions of the AB grains will then be presented, followed by a discussion of the unusual SiC grain M52B-505-1.

### 4.1. AGB stars

During the main sequence phase of the life of a star less massive than ~8 $M_\odot$, core H-burning via the CNO cycles produces $^{13}C$. The products of the CNO cycles are later mixed into the envelope by the "first dredge-up" during the red giant phase, decreasing the surface $^{12}C/^{13}C$ ratio. Following core He-burning, these stars will evolve to the thermally pulsing AGB phase, during which the star is comprised of a C-O core, a He-burning shell, a He intershell, a H-burning shell, and a large convective envelope (Busso et al., 1999). At this stage, the stellar envelope is O-rich. During thermal pulses, shell He-burning produces $^{12}C$. After the pulses, third dredge-up (TDU) occurs where the base of the convective envelope descends to the H- and He-burning regions and brings the nucleosynthetic products, notably $^{12}C$ and the products of *s*-process nucleosyn-

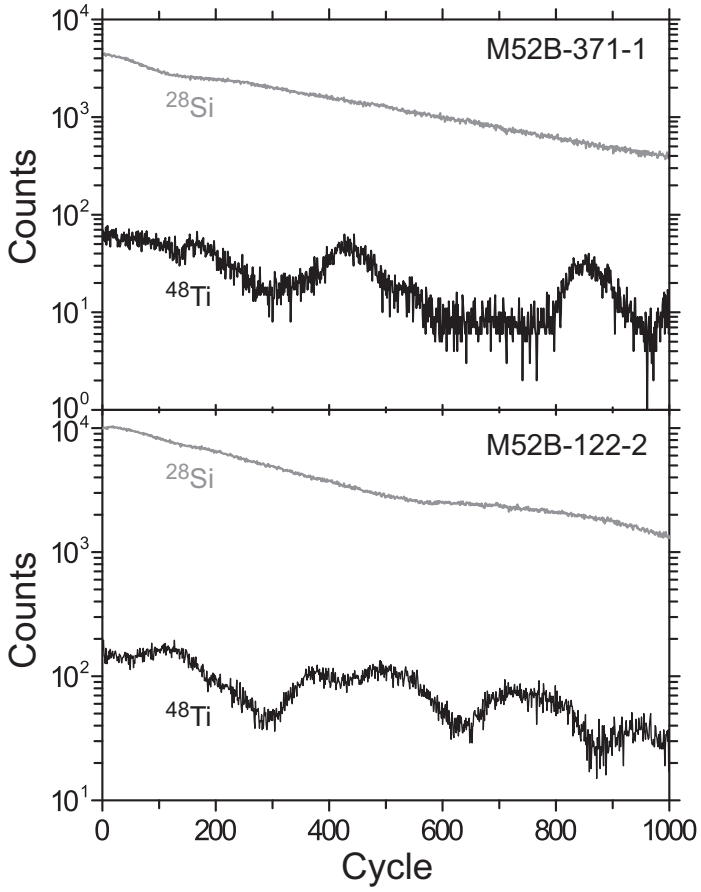


Fig. 5. Change in the counts of $^{28}$Si (in grey) and $^{48}$Ti (in black) during the analyses of grains M52B-371-1 and M52B-122-2. The peaks in the $^{48}$Ti counts are most likely due to the presence of internal TiC grains.

thesis, to the surface of the star. Repeated TDU episodes increase the surface C/O ratio, ultimately producing a C-rich environment that is favorable for the condensation of carbonaceous grains. In intermediate-mass stars ($>\sim$4 $M_\odot$), the base of the envelope becomes hot enough for H-burning reactions to occur, a process termed hot bottom burning (HBB) that prevents the star from becoming C-rich. Thus, SiC grains likely do not originate in such stars. The $^{12}C/^{13}C$ ratios of mainstream SiC grains fall between 10 and 100 (solar $^{12}C/^{13}C = 89$), reflecting the combination of the first dredge-up, which decreases the surface $^{12}C/^{13}C$, and the TDU that then increases the surface $^{12}C/^{13}C$. In addition, a poorly-understood mixing process known as cool bottom processing (CBP) in which envelope material is cycled to regions hot enough for partial H-burning (Nollett et al., 2003; Zinner et al., 2006; Palmerini et al., 2011) may also act to decrease the $^{12}C/^{13}C$ ratio during the AGB phase. On the other hand, Y grains are defined by having $^{12}C/^{13}C > 100$. This is attributed to greater dredge up of $^{12}$C produced during He shell burning compared to the parent stars of mainstream grains. AGB stars of higher mass and/or lower metallicity are predicted to have higher $^{12}C/^{13}C$ ratios and comparisons with models suggest Y grains likely originated in AGB stars of $\sim$half solar metallicity and $\sim$1.5–5 $M_\odot$ (Amari et al., 2001b). Though Z grains likely come from even lower metallicity stars than Y grains based on their Si isotopic ratios (Alexander, 1993; Hoppe et al., 1997; Nittler and Alexander, 2003; Zinner et al., 2006), their $^{13}$C-rich ($^{12}C/^{13}C < 100$) compositions are similar to those of mainstream grains. This has been attributed to CBP occurring more efficiently in lower-metallicity stars and maintaining low $^{12}C/^{13}C$ despite the dredge-up of $^{12}$C (Nittler and Alexander, 2003; Zinner et al., 2006).

Many presolar SiC grains also show clear evidence for having incorporated live $^{26}$Al (half-life $= 7.2 \times 10^5$ yr) in the form of large excesses in $^{26}$Mg. This isotope is produced by shell H-burning in AGB stars and mixed to the surface by the TDU. Its abundance can also be increased by HBB and/or CBP. The inferred $^{26}Al/^{27}Al$ ratios for mainstream, Y and Z grains range from $\sim 3 \times 10^{-5}$ to $2 \times 10^{-2}$ and are in good agreement with AGB nucleosynthesis predictions (Hoppe et al., 1994, 2010; Huss et al., 1997; Amari et al., 2001b; Zinner et al., 2007).

The Si and Ti isotopic compositions are altered in AGB stars by neutron capture reactions occurring in the He intershell. These reactions enhance the abundance of the minor Si and Ti isotopes. The two sources of neutrons are the reactions $^{13}C(\alpha,n)^{16}O$ and $^{22}Ne(\alpha,n)^{25}Mg$. The first reaction occurs in the upper layers of the He intershell

where a $^{13}$C-rich layer, known as the "$^{13}$C pocket", resides. This reaction produces a lower density of neutrons over extended periods of time between thermal pulses. The α-capture reaction on $^{22}$Ne occurs during thermal pulses at the base of the He intershell and produces shorter bursts of neutrons. While Ti isotopes are affected by both neutron sources, the $^{13}$C source results in a marked production of $^{50}$Ti. In general, greater *s*-process shifts in Ti isotopes are expected for low metallicity stars. Neutron capture reactions affect the Ti isotopes to a greater extent than the Si isotopes, which are fueled by the $^{22}$Ne source that is only marginally activated in low-mass AGB stars (Lugaro et al., 1999).

The Si and Ti isotopic compositions of SiC grains, however, cannot be purely explained by models of *s*-process nucleosynthesis in AGB stars. For example, the ranges of isotopic ratios for these elements in mainstream grains are larger than predicted for single AGB stars and the slopes of the correlation lines in isotopic ratio – isotopic ratio plots are distinct from AGB predictions. Instead, these isotope ratios mainly reflect the initial parent stellar compositions as determined by GCE (Alexander, 1993; Gallino et al., 1994; Timmes and Clayton, 1996; Alexander and Nittler, 1999) and possibly local heterogeneities in the ISM (Lugaro et al., 1999; Nittler, 2005). GCE describes the temporal and spatial evolution of the chemical composition of the Galaxy over time. When discussing GCE, it is useful to distinguish "primary" and "secondary" isotopes. The nucleosynthetic yields of primary isotopes are essentially independent of metallicity, whereas secondary isotopes require existing seed nuclei for synthesis. Thus, in general secondary isotopes become more abundant over time relative to primary isotopes, i.e., for Si and Ti the $^{29,30}$Si/$^{28}$Si and $^{46,47,49,50}$Ti/$^{48}$Ti ratios increase with metallicity.

#### 4.1.1. Mainstream SiC grains

We will first discuss the Si and Ti isotopic compositions of mainstream grains, as this will serve as a baseline for the subsequent discussion of the rare types of presolar SiC. The Si isotopic compositions of the mainstream SiC grains fall along a correlation line of slope 1.37 in a plot of $\delta^{29}$Si vs. $\delta^{30}$Si (Fig. 2; Zinner et al., 2007). In contrast, neutron capture reactions in AGB stars produce $^{29}$Si and $^{30}$Si and shift the Si isotopic ratios along a line of slope 0.2–0.5 (Gallino et al., 1994; Lugaro et al., 1999; Amari et al., 2001b; Nittler and Alexander, 2003; Zinner et al., 2006). For low-mass (1–3 $M_\odot$) AGB stars of near solar metallicity, the sources of the mainstream grains, the shifts in the Si isotopic ratios are predicted to be only ~25‰ (Lugaro et al., 1999). The range of Si isotopic ratios of the mainstream grains thus reflects the varying initial parent stellar compositions, which were most likely established by GCE, overprinted by heterogeneous mixing of SN ejecta (Lugaro et al., 1999; Nittler, 2005; Zinner et al., 2006), though more exotic explanations have also been put forward such as a merger of a metal-poor galaxy with the Milky Way (Clayton, 2003). However, the fact that most mainstream grains have $^{29}$Si/$^{28}$Si and $^{30}$Si/$^{28}$Si ratios that are larger than solar implies their parent stars had higher-than-solar metallicities, but were also older than our Sun. This paradox can be explained by the age-metallicity distribution derived for the parent stars of mainstream SiC grains, which indicates that a range of metallicities was present at each stellar age, and that SiC grains condensed more efficiently in higher metallicity stars (Lewis et al., 2013).

The Ti isotopic compositions of mainstream grains behave in a similar fashion to the Si isotopes, where the ranges of compositions and slopes on three-isotope plots cannot be explained solely by AGB nucleosynthesis (Lugaro et al., 1999). The Ti isotopic compositions of the mainstream SiC grains from this study fall in the ranges observed in other studies (Hoppe et al., 1994; Alexander and Nittler, 1999; Amari et al., 2001b, 2001c; Gyngard et al., 2006; Huss and Smith, 2007; Zinner et al., 2007). The $\delta^{47}$Ti/$^{48}$Ti and $\delta^{46}$Ti/$^{48}$Ti values show a tight correlation (Fig. 3) that is close to the trends predicted by GCE models (Timmes et al., 1995; Alexander and Nittler, 1999; Zinner et al., 2007). The spread in the data along the correlation line thus likely reflects the variable initial Ti isotopic compositions of the parent stars. The $\delta^{49}$Ti/$^{48}$Ti values of the mainstream grains in this study are also correlated with $\delta^{46}$Ti/$^{48}$Ti, though some grains from the literature show small enhancements in $^{49}$Ti from *s*-process nucleosynthesis and TDU. Assuming that the overall GCE trend passes through the solar composition (i.e., $\delta^{i}\mathrm{Ti} = 0$), this AGB contribution pushes the intercept of the correlation line in the $\delta^{49}$Ti vs. $\delta^{46}$Ti plot to a positive value. Indeed, the mainstream correlation line in this plot has a positive intercept. Clearly deviating from the GCE trend are the $^{50}$Ti enrichments observed in a proportion of the grains. As noted by Zinner et al. (2007), stars of ~solar metallicity are not expected to experience a large degree of neutron capture nucleosynthesis. In principle, the large spread in $\delta^{50}$Ti/$^{48}$Ti values could be explained by the heterogeneous distribution in interstellar space of $^{50}$Ti, which is produced mainly in a rare subset of Type Ia SNe rather than in Type II SNe as the other Ti isotopes are (Meyer et al., 1996; Woosley, 1997). Contributions from Type Ia SNe are more significant in the later stages of GCE. The GCE of the Si isotopes based on SiC grain data indicate a strong contribution of $^{28}$Si from Type Ia SNe in the late phase of Galactic evolution (Amari et al., 2001b; Zinner et al., 2006). However, that we observe enhancements in $^{49}$Ti, which is not produced in Type Ia SNe but is more likely a product of neutron capture reactions, indicates that a portion, if not all, of the excess $^{50}$Ti observed in the mainstream grains is due to AGB nucleosynthesis. Activation of the $^{13}$C neutron source in the parent AGB stars greatly enhances the $^{50}$Ti abundance in the He intershell. Moreover, $^{50}$Ti is neutron magic and has a small neutron capture cross section and large nuclear binding energy relative to the other Ti isotopes, which can result in accumulation of this isotope.

The Ti and Si isotopic compositions for succeeding TDU episodes predicted by the AGB nucleosynthesis models of Cristallo et al. (2011) for 1.5 $M_\odot$ and 3 $M_\odot$ stars of metallicities 0.014 (solar), 0.006, and 0.003 are plotted in Figs. 3 and 4. The solar Ti and Si isotope abundances were taken from Asplund et al. (2009). The results are scaled so that the initial isotopic ratios for each metallicity are the

values used by Zinner et al. (2007). The initial isotopic ratios in that study were determined by assuming that the abundances of the primary isotopes increased according to observations of thin- and thick-disk stars and that the abundances of secondary isotopes scaled with the Fe abundance. The derived initial $\delta^{i}$Ti was -260‰ for Z=0.006 and -378‰ for Z=0.003, and the initial $\delta^{29}$Si was -113‰ for Z=0.006 and -173‰ for Z=0.003. For stars of 1.5 $M_{\odot}$ and Z=0.014, the AGB model indicates an increase in $\delta^{49}$Ti of ~50‰ and $\delta^{50}$Ti of ~90‰. The predicted $^{49}$Ti and $^{50}$Ti enrichments are consistent with the isotopic compositions of 7 and 4 of our mainstream SiC grains, respectively, with the other grains having larger enrichments. For 3 $M_{\odot}$ stars and Z=0.014, $\delta^{49}$Ti is predicted to increase by ~150‰ and $\delta^{50}$Ti by ~240‰ relative to the starting composition. These values are consistent with the measured $^{49}$Ti and $^{50}$Ti enhancements observed in some mainstream SiC grains. As will be discussed in section 4.2, the AB grain data also support AGB nucleosynthesis as the cause of the $^{49}$Ti and $^{50}$Ti enhancements observed in the mainstream grains.

The Si and Ti isotopic compositions of the mainstream SiC grains are highly correlated, providing further evidence that both elements are greatly affected by GCE (Hoppe et al., 1994; Alexander and Nittler, 1999; Nittler, 2005). In Fig. 4, the Ti isotopic ratios of the grains from this study are plotted against the $^{29}$Si/$^{28}$Si ratios along with the least square fits to the isotopic ratios of ~300 mainstream SiC grains from the literature. Comparisons with the $^{30}$Si/$^{28}$Si ratios are not made because AGB nucleosynthesis produces larger enhancements in $^{30}$Si than $^{29}$Si, especially at lower metallicities. Also plotted are the AGB model predictions of Cristallo et al. (2011) that show that the $\delta^{29}$Si values are barely affected by AGB nucleosynthesis. The mainstream grains from this study generally fall along the correlation lines. However, the two grains with the largest $\delta^{29}$Si values, M52B-596–3 and M52B-723–1 (labeled in Fig. 4), plot well below the mainstream lines for $\delta^{46}$Ti, $\delta^{49}$Ti, and $\delta^{50}$Ti vs. $\delta^{29}$Si. The $\delta^{49}$Ti and $\delta^{50}$Ti values of these grains are close to those of AB grains, and this could indicate their parent stars did not undergo appreciable *s*-process nucleosynthesis. However, the low $\delta^{46}$Ti values are difficult to explain especially given the fact that the $\delta^{47}$Ti values plot close to the mainstream correlation line. On the other hand, the Ti isotopic compositions of these two grains are within 3σ error of solar, so it is possible that the measurements of these grains suffered from terrestrial contamination. Grain M52B-750–1 also plots far below the mainstream correlation lines with a more $^{48}$Ti-rich composition than other mainstream grains, but similar isotopic compositions to AB grains. It is possible that the parent star of this grain did not undergo significant *s*-process nucleosynthesis. Excluding these grains, the data follow the mainstream correlation lines for $\delta^{49}$Ti and $\delta^{50}$Ti vs. $\delta^{29}$Si. For $\delta^{46}$Ti and $\delta^{47}$Ti vs. $\delta^{29}$Si, our mainstream data appear to show a shallower slope than the literature correlation lines. However, the data plot in the same range as the mainstream grains from the literature (Hoppe et al., 1994; Alexander and Nittler, 1999; Gyngard et al., 2006; Huss and Smith, 2007; Hynes and Gyngard, 2009), and given the small number of grains measured here the discrepancy in the slope is probably not significant. Note that the mainstream correlation lines have positive intercepts in the $\delta^{49}$Ti and $\delta^{50}$Ti vs. $\delta^{29}$Si plots, which agrees with the model predictions of AGB contributions for $^{49}$Ti and especially $^{50}$Ti in stars of ~solar metallicity.

#### 4.1.2. Y Grains

The Si isotopic compositions of many of the Y grains plot to the right of the mainstream correlation line on a plot of $\delta^{29}$Si vs. $\delta^{30}$Si (Fig. 2) and largely follow a trend line that has a shallower slope than for the mainstream grains. These observations are attributed to the initial compositions of the Y grains' parent stars and the contribution from AGB nucleosynthesis. Based on comparisons of major- and minor-element isotopic compositions with AGB models, the parent stars of Y grains had lower initial $^{29}$Si/$^{28}$Si and $^{30}$Si/$^{28}$Si ratios than the parent stars of the mainstream grains and are inferred to have come from ~1/2 solar metallicity AGB stars (Amari et al., 2001b). The initial Si-isotope ratios of the Y grain parent stars can be estimated by subtracting the AGB contribution and projecting the measured ratios back onto the GCE line. The exact position of this line is not known. Theoretical models predict a line of slope 1 going through the solar composition ($\delta^{i}Si = 0$) (e.g., Timmes and Clayton, 1996), but the mainstream correlation line of slope ~1.37 has also been used as an estimate of the GCE of Si (Amari et al., 2001b; Zinner et al., 2006). Note however that the Si isotopic ratios of the mainstream SiC grains are affected to some extent by AGB nucleosynthesis and subtracting this AGB contribution would shift the mainstream correlation line to the left by ~20‰. The initial Si isotopic compositions of the Y grains determined by projecting the measured isotopic ratios onto the shifted (AGB corrected) mainstream correlation line would be more $^{28}$Si-rich than if they were projected onto the uncorrected correlation line. As will be discussed in Section 4.2, the AB grain correlation line for Si isotopes may provide a better estimation of the GCE of Si.

AGB nucleosynthesis enhances $^{29}$Si and $^{30}$Si through neutron capture reactions and the stellar envelopes of low metallicity AGB stars are more enriched in the products of these reactions. These stars have higher temperatures in their He shells, generate more neutrons, and experience dredge up to greater depths. Moreover, the envelopes of low metallicity stars have lower initial abundances of elements including C, Si, and Ti, and there is consequently less dilution of dredged-up material. Y grains, therefore, generally have greater enhancements in $^{29}$Si and $^{30}$Si than are observed in mainstream SiC grains, which is consistent with their higher $^{12}$C enhancements. However, the Si isotope ratios of many of the Y grains overlap those of the mainstream grains, especially for the more $^{28}$Si-rich grains. The tighter distribution of Si isotopic compositions of the Y grains indicates that the number of Y grain parent stars is fewer than the parent stars of mainstream grains and that they had a smaller range of initial isotopic compositions. Amari et al. (2001b) estimated that fewer than 10 parent stars are needed to explain the Y grain data. The larger scatter in the Si isotopic ratios of the mainstream SiC grains

is likely due to a wider range of parent stellar compositions and greater degree of local heterogeneity in the material that formed these stars.

Y grains are also expected to have greater enhancements in $^{50}$Ti and perhaps also $^{49}$Ti from neutron capture reactions than mainstream grains. Previously, only 23 Y grains had been analyzed for their Ti isotopic compositions (Amari et al., 2001b; Zinner et al., 2007). The Ti isotopic compositions of the Y grains from our study overlap those of mainstream grains in plots of $\delta^{47}$Ti and $\delta^{49}$Ti versus $\delta^{46}$Ti (Fig. 3). Unlike the Si isotopes, AGB nucleosynthesis does not appear to affect these Ti isotopes more in half solar metallicity stars than in solar metallicity stars. The AGB models for 1.5 $M_\odot$ and 3 $M_\odot$ stars of $Z = 0.01$ predict enhancements in $^{49}$Ti of ~60‰ and ~140‰, respectively (Cristallo et al., 2011). These enhancements are about the same for stars of $Z = 0.014$. The similar $\delta^{49}$Ti values of Y and mainstream grains are in agreement with the AGB models. Moreover, the degree of $^{49}$Ti enrichment measured in the Y and mainstream grains is comparable to the values predicted in these models. The Y grains show a wider range of $\delta^{50}$Ti values compared to mainstream grains, with ~30% of the Y grains having greater enhancements in $^{50}$Ti than the mainstream grains. For example, grain M52B-385-4 shows an extremely high $\delta^{50}$Ti of $510 \pm 9$‰ though the $\delta^{30}$Si value is unremarkable. These compositions point to the strength of the $^{13}$C neutron source in the parent star of M52B-385-4. Only the Y grain KJGM1-158-5 has a larger $^{50}$Ti enhancement ($990 \pm 55$‰) and also is more $^{30}$Si-rich (Amari et al., 2001b). The AGB models for 1.5 $M_\odot$ and 3 $M_\odot$ stars of $Z = 0.01$ predict enhancements in $^{50}$Ti of ~150‰ and ~275‰, respectively (Cristallo et al., 2011). For stars of $Z = 0.014$, the predicted $^{50}$Ti enrichments are ~90‰ and ~240‰ for 1.5 $M_\odot$ and 3 $M_\odot$, respectively (Cristallo et al., 2011). These models thus predict greater $^{50}$Ti enrichments in the parent stars of Y grains than mainstream grains, and the grain data are in agreement with these predictions. Moreover, the degree of $^{50}$Ti enrichments from the initial compositions in the models agrees with the grain data, though a few Y grains show greater enrichments.

The $\delta^{46}$Ti, $\delta^{47}$Ti, and $\delta^{49}$Ti values of the Y grains all show correlations with $\delta^{29}$Si, though they are not as tight as for other grain types (Fig. 4). Grains with negative $\delta^{29}$Si values appear to have more scatter in their Ti isotopic compositions, but the range of compositions is similar to that observed for the Y grains in the literature and mainstream grains. The $\delta^{50}$Ti compositions are not well correlated with $\delta^{29}$Si, again reflecting the prominence of AGB nucleosynthesis affecting $^{50}$Ti but not $^{29}$Si. The projected initial $\delta^{29}$Si values of the parent stars of Y grains are lower than for mainstream grains and indicate low metallicity stellar sources. As previously noted, the $\delta^{46}$Ti and $\delta^{47}$Ti values do not appear to be highly affected by AGB nucleosynthesis and AGB models predict enrichments in $^{46}$Ti and $^{47}$Ti to be less than 30‰ and 6‰, respectively. If the $\delta^{46}$Ti and $\delta^{47}$Ti values mainly reflect GCE, then these values should also be lower than for mainstream grains. Though the statistics are still limited for Y grains, the intercepts of the correlation lines for these grains do not appear to differ much from the mainstream correlation lines. This suggests that the $^{46}$Ti/$^{48}$Ti and $^{47}$Ti/$^{48}$Ti ratios did not evolve rapidly in the Galaxy after the time that the Y grain parent stars formed.

#### 4.1.3. Z Grains

The type Z SiC grains have relatively large $^{30}$Si enrichments and all but one of the grains studied here have lower $\delta^{29}$Si values than the Y grains (Fig. 2). These typical Z grain characteristics have been used to argue that Z grains originated in roughly one third solar metallicity AGB stars that had lower initial $^{29}$Si/$^{28}$Si and $^{30}$Si/$^{28}$Si ratios than the parent stars of Y grains. These stars also experienced a much greater degree of *s*-process nucleosynthesis than the parent stars of Y grains and consequently have larger $^{30}$Si enrichments.

The 9 Z grains in this study show a very similar range of Ti isotopic compositions to the 11 Z grains discussed previously by Zinner et al. (2007). In the plots of $\delta^{47}$Ti and $\delta^{49}$Ti versus $\delta^{46}$Ti, the Z grains fall along the mainstream correlation lines but extend the trends to more negative values (Fig. 3). This corroborates the low metallicity stellar sources for these grains. Moreover, the trends provide further evidence that the $^{46,47,49}$Ti isotopes in AGB-derived SiC grains are mainly influenced by GCE. The AGB models for $Z = 0.006$ and $Z = 0.003$ plot parallel to the mainstream correlation line in the plot of $\delta^{47}$Ti vs. $\delta^{46}$Ti, but it is clear that the assumed initial Ti isotopic compositions are shifted down and miss the grain data. AGB nucleosynthesis does not affect the $^{46}$Ti or $^{47}$Ti abundances to a large degree and the spread in the Z grain data along the correlation line likely denotes the varying initial isotopic compositions of their parent stars. In the plot of $\delta^{49}$Ti vs. $\delta^{46}$Ti, the assumed initial ratios fall very close to the mainstream correlation line and the degree of $^{49}$Ti enrichment predicted by the AGB nucleosynthesis models approximately covers the range of $\delta^{49}$Ti values measured for the Z grains. The Z grains show large positive deviations from the mainstream correlation line in the plot of $\delta^{50}$Ti vs. $\delta^{46}$Ti. The degree of $^{50}$Ti enrichment is greater than that for Y grains, again demonstrating the increased level of *s*-process nucleosynthesis as the stellar metallicity decreases. The AGB models predict lower $^{50}$Ti enrichments than measured in many of the Z grains, especially if the initial $\delta^{50}$Ti values are shifted down to the mainstream correlation line. This suggests that the dosage of $^{13}$C used in the models is too low and a higher neutron flux is required to match the grain data.

Similar to the Y grains, the $\delta^{46}$Ti, $\delta^{47}$Ti, and $\delta^{49}$Ti values of the Z grains show a correlation with $\delta^{29}$Si (Fig. 4). The Z grains extend the mainstream correlation lines to negative $\delta^{i}$Ti and $\delta^{29}$Si values, consistent with origins in low metallicity AGB stars, but they generally plot below the mainstream correlation lines. While the correlation line for the Z grains in the $\delta^{47}$Ti vs. $\delta^{29}$Si plot lies parallel to the mainstream correlation line, they are steeper in the $\delta^{46,49}$Ti vs. $\delta^{29}$Si plots. The fact that these grains lie below the correlation lines for mainstream and Y grains and that the slopes of some of the Z grain correlation lines are different could indicate the GCE of the Si and Ti isotopes evolve differently at low metallicities. The steeper slopes of the Z grain corre-

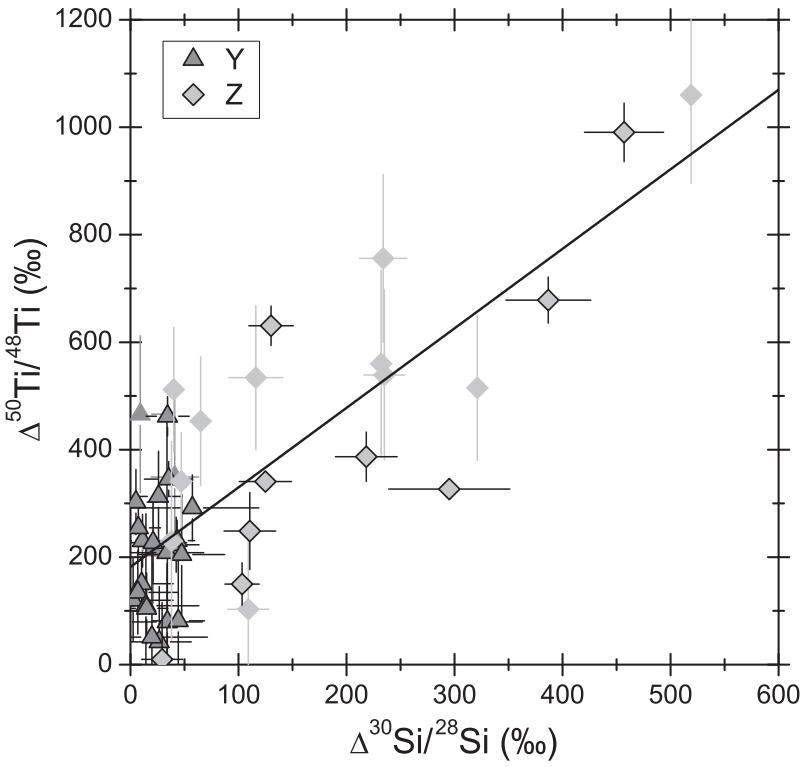


Fig. 6. Isotopic shifts due to AGB nucleosynthesis in the $^{50}Ti/^{48}Ti$ and $^{30}Si/^{28}Si$ ratios in permil (‰) of SiC grains of types Y and Z. These shifts are due to AGB nucleosynthesis. Grains from this study are outlined in black. Also plotted are data from Zinner et al. (2007). The line is the fit to all data points ($\Delta^{50}Ti/^{48}Ti = 1.48 \times \Delta^{30}Si/^{28}Si + 181.8$).

lations indicate curvature in the Ti-Si GCE trends. This would suggest that the secondary Ti isotopes were evolving more rapidly than the secondary Si isotopes at the time the parent stars of the Z grains were forming. The shallower slope of the Z grain correlation line in $\delta^{47}Ti$ vs. $\delta^{29}Si$ relative to the other Z grain correlation lines suggests $^{47}Ti$ did not evolve as rapidly when the Z grain parent stars were forming, but the material from which the stars formed was more enriched in $^{47}Ti$ than the other Ti isotopes. The AGB models lie close to the grain data for $\delta^{46,49}Ti$ vs. $\delta^{29}Si$, indicating the assumed initial $\delta^{46}Ti$, $\delta^{49}Ti$, and $\delta^{29}Si$ values at low metallicities are reasonable. However, the assumed initial $\delta^{47}Ti$ ratios at low metallicities should be increased. The large excesses of $^{50}Ti$ observed in the Z grains are again due to the prominence of n-capture reactions in lower metallicity stars. The $^{49}Ti$ and $^{50}Ti$ enrichments in some of the grains are greater than the AGB model predictions, but the degree of this discrepancy depends on the initial isotopic compositions.

In Fig. 6, the isotopic shifts in $^{50}Ti/^{48}Ti$ and $^{30}Si/^{28}Si$ due to AGB nucleosynthesis are plotted for Y and Z grains from this study and from Zinner et al. (2007). These values were determined in the manner employed by Amari et al. (2001b), Nittler and Alexander (2003), Zinner et al. (2006) and Zinner et al. (2007). The isotopic compositions of the grains were projected along the modeled paths of AGB nucleosynthesis onto the GCE lines, assumed to be the mainstream correlation lines. The slope used for the AGB nucleosynthesis path for $\delta^{29}Si$ vs. $\delta^{30}Si$ was 0.16, which is the average slope for 1.5 and 2 $M_\odot$ AGB models at $Z = 0.006$ and 0.003 (see Zinner et al., 2006). For the $\delta^{50}Ti$ vs. $\delta^{46}Ti$ AGB path, the average of 1.5 $M_\odot$ AGB models at $Z = 0.006$ and 0.003 gave a slope of 12.5. The deviation of the measured ratio from this "initial" ratio is taken to be the contribution from AGB nucleosynthesis. The fit through all the data points has a slope of ~1.5 and an intercept of ~180‰. The shifts in $^{50}Ti$ are larger than for $^{30}Si$, especially for Y grains. The $\Delta^{50}Ti/^{48}Ti$ and $\Delta^{30}Si/^{28}Si$ values span ~400‰ and 50‰, respectively, for the Y grains. For the Z grains, the $\Delta^{50}Ti/^{48}Ti$ and $\Delta^{30}Si/^{28}Si$ values span ~1000‰ and 400‰, respectively. This indicates that the $^{13}C$ source produces a greater total fluence of neutrons than the $^{22}Ne$ source in the low metallicity parent stars of both Y and Z grains. The Z grains generally display greater enhancement of $^{50}Ti$ and $^{30}Si$ from AGB nucleosynthesis than the Y grains. However, the isotopic shift in $^{30}Si/^{28}Si$ relative to $^{50}Ti/^{48}Ti$ is ~3 times greater in Z grains than in Y grains. This is due to the higher temperatures at the base of the He shell in the parent stars of Z grains, causing the $^{22}Ne$ source to produce more neutrons. Moreover the depth of the TDU is greater in these stars.

### 4.2. AB grains

#### 4.2.1. Proposed stellar sources

The stellar sources of AB grains have been enigmatic and their isotopic properties cannot be reproduced by cur-

rent stellar models. AB grains have Si isotopic compositions that overlap the compositions of mainstream SiC grains (Fig. 2). These grains are distinguished from the mainstream grains by having low $^{12}C/^{13}C$ (<10) ratios, which are likely a consequence of the CNO cycle. Stellar envelopes become C-rich from the production of $^{12}C$ during He-burning and subsequent repeated TDU. It is under these C-rich conditions that SiC grains can condense. The TDU also increases the $^{12}C/^{13}C$ in the envelope to the values observed in mainstream SiC grains (~10 to 100). In order for AB SiC grains with low $^{12}C/^{13}C$ ratios to condense, their parent stellar source(s) had to have experienced H-burning to produce $^{13}C$ after the star became C-rich. The N isotopic compositions of AB grains cover the range of mainstream grains (i.e., $^{14}N/^{15}N$ ~terrestrial up to ~$10^4$), but a significant fraction (~30%) also extend to lower-than-solar $^{14}N/^{15}N$ ratios. Alexander (1993) and Amari et al. (2001c) proposed that the two most likely stellar sources of AB grains are born-again AGB stars or J-type carbon stars. Spectroscopic observations indicate that these C-rich stars have low $^{12}C/^{13}C$ ratios (<~10) similar to those of AB grains (Lambert et al., 1986; Asplund et al., 1999; Ohnaka and Tsuji, 1999).

Born-again AGB stars, such as Sakurai's object, are in the post-AGB phase and have lost most of their envelope. These stars undergo a very late thermal pulse that generates abundant $^{12}C$ (Asplund, 1999; Herwig, 2001). The convective He shell extends into the remaining H envelope, and convective H-burning of $^{12}C$ produces $^{13}C$ and low $^{12}C/^{13}C$ ratios (Herwig et al., 2011). These stars also show *s*-process element enrichments, indicating activation of the $^{13}C$ neutron source (Kipper and Klochkova, 1997; Asplund et al., 1999; Herwig et al., 2011).

In contrast to born-again AGB stars, J-type carbon stars do not show enhancements in *s*-process elements (Utsumi, 1985; Abia and Isern, 2000). The mechanism for $^{13}C$ enrichment, if it occurred via thermal pulses, without the occurrence of neutron capture reactions remains unknown. These stars also have $^{14}N/^{15}N$ ratios consistent with those measured in AB grains, including grains with low $^{14}N/^{15}N$ ratios (Hedrosa et al., 2013). The formation of these stars is unfortunately not well understood. Possible scenarios include an extra mixing mechanism such as CBP, mixing at the He-core flash, and binary systems (see Ohnaka and Tsuji, 1999; Abia and Isern, 2000; Amari et al., 2001c).

Type II SNe have also been tentatively suggested as the stellar sources of some AB grains. One AB grain was found to have enhancements in *r*- and *p*-process isotopes of Mo and Ru (Savina et al., 2003, 2007). A possible location for production of *p*-process isotopes is Type II SN. However, the SN models predict greater *p*-process isotope enhancements than observed in the grain, and the C and Si isotopic compositions of these grains were not compatible with SN origins. Savina et al. (2007) thus proposed mixing of SN material with isotopically solar material in a binary system. However, the mixing calculations could not reproduce all measured isotopes of this grain. Three AB grains were found to have $^{32}S$ enhancements (Fujiya et al., 2013). Though this isotopic signature could result from the Si/S zone of a SN, the C and Al isotopic compositions of these grains do not fit a SN origin. The authors suggested born-again AGB stars as the sources of these grains. Some $^{15}N$-rich AB grains also have enrichments in $^{32}S$ and $^{50}Ti$, suggestive of proton and neutron capture reactions in Type II SNe (Nittler et al., 2016).

#### 4.2.2. Ti and Si isotopic compositions of AB grains

45 AB grains were analyzed previously for their Ti isotopic compositions (Ireland et al., 1991; Virag et al., 1992; Hoppe et al., 1994; Amari et al., 2001c; Gyngard et al., 2006; Zinner et al., 2007). The 26 AB grains in this study have Ti isotopic compositions that are similar to previous analyses. The Ti isotopic ratios closely follow the mainstream correlation lines and cover approximately the same range of compositions (Fig. 3). This suggests that the grains derived from stars of close to solar metallicity. One notable difference is that the AB grains do not show enhancements in $^{50}Ti$ as do other SiC grains from AGB stars. Note that the mainstream grains from this study have moderate $^{50}Ti$ enrichments, but the mainstream grains reported in the literature have $\delta^{50}Ti$ values ranging up to ~450‰. As noted previously, the $^{50}Ti$ enrichments observed in some mainstream grains could have resulted from AGB nucleosynthesis or heterogeneous distribution of $^{50}Ti$ in interstellar space, or a combination of the two. If AB grains derived from stars of ~solar metallicity, then they formed at approximately the same time as mainstream grains. If there was a heterogeneous distribution of $^{50}Ti$ in the Galactic disk during this time, this would imply that the AB grains sampled a discrete location that had a more homogeneous distribution of $^{50}Ti$. This explanation is tentative, however, and it is more likely that the parent stars of AB grains did not experience extensive dredge-up of the products of *s*-process nucleosynthesis.

The Ti isotopic compositions of the AB grains are correlated with $\delta^{29}Si$ and follow along the mainstream correlation lines (Fig. 4). However, the $^{50}Ti/^{48}Ti$ and to a lesser extent the $^{49}Ti/^{48}Ti$ and $^{46}Ti/^{48}Ti$ ratios of most of the grains fall below the mainstream correlation lines. This indicates again that the parent stars of AB grains underwent significantly less dredge-up of *s*-process nucleosynthesis products than did the mainstream parent stars. The Ti isotopic compositions of the AB grains thus support an origin in J-type C stars. The mainstream grains have higher $\delta^{50}Ti$ values than expected for near-solar metallicity stars and are likely more affected by *s*-process nucleosynthesis than previously thought. If this is the case, then AB grains provide a better model for GCE. Indeed, the intercept of the fits to the AB grain Ti isotopic ratios are closer to the solar compositions ($\delta^{i}Si = \delta^{i}Ti = 0$). The Si isotopic compositions of the AB grains may also provide a better measure of GCE. The contributions from AGB nucleosynthesis in mainstream grains would shift the grain compositions in the $\delta^{29}Si$ vs. $\delta^{30}Si$ plot from their initial compositions along the true GCE line to the right and produce a shallower slope. The true GCE line would, therefore, have a steeper slope and more positive intercept than the mainstream correlation line. The correlation line for all AB grains has a slightly shallower slope than the

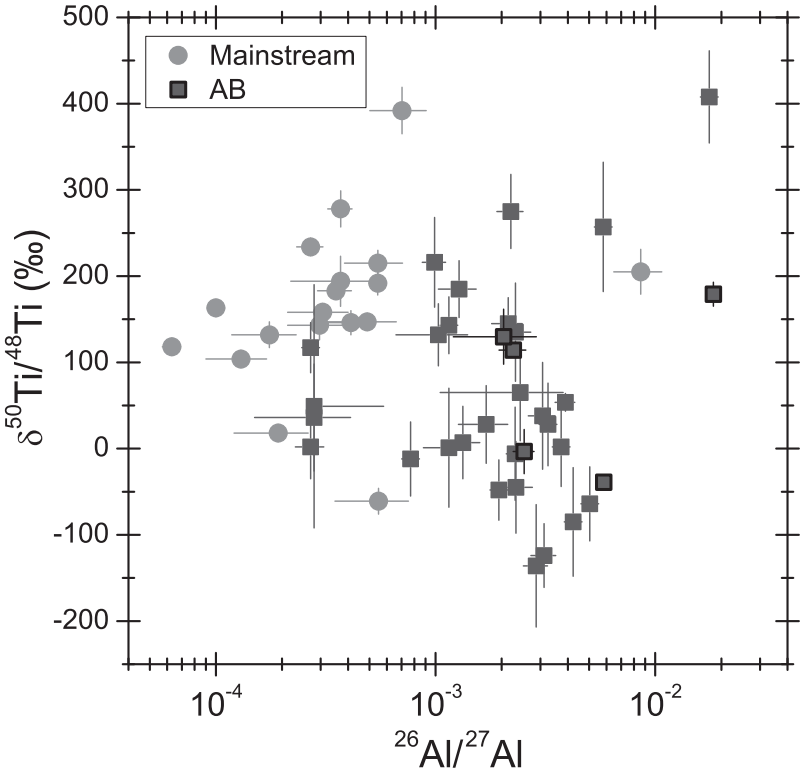


Fig. 7. $^{50}Ti/^{48}Ti$ and inferred $^{26}Al/^{27}Al$ ratios of AB and mainstream grains. The AB grains generally have lower $^{50}Ti/^{48}Ti$ and higher $^{26}Al/^{27}Al$ ratios than mainstream grains. Grains reported in this study are outlined and data from other studies are from Virag et al. (1992), Hoppe et al. (1994), Amari et al. (2001c) and Zinner et al. (2007).

mainstream correlation line. However, we find that the Si isotope correlation line for AB grains with $^{14}N/^{15}N$ ratios greater than solar differs from that of AB grains with $^{14}N/^{15}N$ ratios lower than solar. The correlation line for AB grains having $^{14}N/^{15}N >$ solar has a slope and intercept that are within error of those of the mainstream correlation line, while the $^{15}N$-rich AB grains show a shallower slope (~0.9). This difference stems from the fact that these two grain populations likely have different stellar sources. At least some of the $^{15}N$-rich AB grains likely come from Type II SNe (Nittler et al., 2016), and their Si isotopic ratios would not necessarily reflect GCE. On the other hand, the $^{14}N$-rich AB grains trace the GCE of Si with some contribution from AGB nucleosynthesis, similar to the mainstream grains. Of course, some of these $^{14}N$-rich AB grains have enhancements in $^{50}Ti$ and thus greater *s*-process contributions than grains that do not have $^{50}Ti$ enrichments. The $^{14}N$-rich grains that are not enriched in $^{50}Ti$ likely provide a better estimation of the initial Si and Ti isotopic compositions, but the statistics for these grains are still limited.

#### 4.2.3. $^{26}Al/^{27}Al$ isotopic compositions

In Fig. 7, the $\delta^{50}Ti$ values of mainstream and AB grains are plotted against inferred $^{26}Al/^{27}Al$ ratios for presolar SiC grains. Aluminum-26 is produced in the H-burning shell and brought to the stellar envelope by dredge-up episodes. However, it is produced more extensively during CBP. The $^{26}Al/^{27}Al$ ratios of AB grains from this study and others (Virag et al., 1992; Hoppe et al., 1994; Amari et al., 2001c; Zinner et al., 2007) are generally larger than in mainstream grains. Some of these AB grains also have $^{50}Ti$ excesses and could come from born-again AGB stars. The parent stars of AB grains having high $^{14}N/^{15}N$ ratios likely underwent CBP. For the grains that do not show enhancements in $^{50}Ti$, H-burning in J stars likely produced the high $^{26}Al/^{27}Al$ ratios and low $^{12}C/^{13}C$ ratios. As has been discussed by Amari et al. (2001c), a difficulty with this scenario is that H-burning not only produces $^{13}C$ but also converts C to N and reduces the C/O ratio. So there must be a balance between He-burning to produce $^{12}C$ and H-burning.

#### 4.2.4. Probable stellar source of AB grains in this study

The lack of *s*-process enhancement of the Ti isotopes and high $^{26}Al/^{27}Al$ ratios in the AB grains in this study lends support to J stars as the stellar sources. Moreover, nucleosynthesis models of born-again AGB stars predict large enhancements in $^{29}Si$ and $^{30}Si$ in the He intershell ($\delta^{29}Si = 2100‰$ and $\delta^{30}Si = 9500‰$) (Herwig et al., 2011). Such extreme Si isotopic compositions have not been observed in AB grains and large dilution of the Si isotopes with isotopically normal material would need to be invoked to explain the grain data. However, as previously mentioned, some AB grains do have *s*-process enrichments that suggest they could have derived from born-again AGB stars (Amari et al., 2001c). Some presolar high density (HD)

graphite grains also have low $^{12}C/^{13}C$ ratios that are similar to those of AB grains. Some of these HD graphite grains were found to have extremely anomalous Ca and Ti isotopic compositions that can be explained by He shell nucleosynthesis in born-again AGB stars (Jadhav et al., 2008, 2013). The Ti isotopic anomalies greatly exceed those measured in presolar SiC grains, however. Recently, three AB grains were found to have excesses in $^{32}S$ that could have derived from radioactive $^{32}Si$ (half-life = 153 yr) produced in born-again AGB stars (Fujiya et al., 2013), but these authors had to invoke extensive dilution with isotopically normal material to explain the lack of large Si-isotopic anomalies.

### 4.3. Grain M52B-505-1

As mentioned in Section 3, a highly $^{30}Si$-enriched grain, M52B-505-1, was identified by the automated Si- and C-isotopic measurements (Fig. 1). The $\delta^{30}Si$ value of ~850‰ for this grain is similar to that reported for some putative nova SiC grains (Amari et al., 2001a) and to an unclassified grain, M26a-454-3, reported by Nittler and Alexander (2003). Like that grain, M52B-505-1 has isotopically light C and close to normal or slightly enriched $^{29}Si$. The light C argues against a nova origin since nova nucleosynthesis produces C with very low $^{12}C/^{13}C$ ratios. Another class of SiC grains with large $^{30}Si$ excesses, C grains (Liu et al., 2016 and references therein), derives from SNe, but these grains are also characterized by very large $^{29}Si$ excesses that are not observed in grains M26a-454-3 or M52B-505-1. We measured M52B-505-1 for its N isotopic composition and found that it has a $^{14}N/^{15}N$ ratio of ~3800, similar to those seen in the mainstream SiC grains and predicted for AGB star envelopes. The C, Si and N isotopes for this unusual grain may point to an origin in a very low-metallicity star that originated with isotopically light Si, but for which extensive dredge-up of *s*-process material led to the observed composition. Unfortunately, we were unable to measure this grain for Ti isotopes, which could have been diagnostic. Multi-element isotopic analysis of additional such grains found in the future will help to constrain their origins.

## 5. CONCLUSIONS

We have expanded the number of rare types of SiC grains for which multi-element isotopic analyses including Ti have been performed. The Ti isotopic ratios of the grains are generally correlated with $^{29}Si/^{28}Si$, indicating a great influence of GCE on these isotopic ratios. Many of the AGB-derived grains showed enrichments in $^{50}Ti$ and also $^{49}Ti$, which are products of *s*-process nucleosynthesis. The AGB models of Cristallo et al. (2011) are generally consistent with the grain data. However, the $^{49}Ti$ and $^{50}Ti$ enhancement in some Y and Z grains are greater than predicted, suggesting a greater neutron dosage from the $^{13}C$ source.

We find that mainstream SiC grains have greater *s*-process enhancements than previously thought. The enhancements predicted by models of AGB nucleosynthesis for stars of solar metallicity, the parent stars of mainstream grains, are consistent with the grain data. The similarity in the $^{46}Ti/^{48}Ti$ and $^{47}Ti/^{48}Ti$ isotopic ratios of the Y grains and mainstream grains suggests that these ratios did not evolve rapidly in the Galaxy after the time that the parent stars of Y grains formed. The Ti isotopic ratios of the Z grains indicate that the Ti isotopes evolved more rapidly and perhaps non-linearly at low metallicities. The Z grain data also suggest that $^{47}Ti$ evolved less rapidly than the other secondary Ti isotopes at the time the parent stars of Z grains formed, but that the initial abundance was greater than the other Ti isotopes.

The AB grains in this study did not show enhancements in *s*-process isotopes and these grains likely derived from J-type C stars rather than born-again AGB stars. The AB grains have high $^{26}Al/^{27}Al$ ratios and low $^{12}C/^{13}C$ ratios that are likely the result of H-burning in J stars. Some of the AB grains are less affected by AGB nucleosynthesis than mainstream SiC grains (i.e., grains that do not have $^{50}Ti$ enrichments), and their correlation lines for Si and Ti isotopes are likely better representations of the true GCE of these isotopes.

Evidence for internal TiC grains were found in all of the presolar SiC grain types analyzed in this study. Similar proportions of the Y and Z grains contained internal TiC subgrains (~39% on average), while the mainstream and AB grains had lower abundances of TiC subgrains (~21% on average). The Y and Z grains also had higher concentrations of Ti than the mainstream and AB grains. These observations point to the different chemical compositions of the low metallicity parent stars of Y and Z grains compared to the ~solar metallicity parent stars of mainstream and AB grains.

The automated mapping of 2700 SiC grains revealed one very rare $^{12}C$- and $^{30}Si$-rich grain. The grain's normal $^{29}Si/^{28}Si$ ratio and mainstream-like $^{14}N/^{15}N$ ratio suggest an origin in a very low-metallicity AGB star. Multi-element isotope data for similar grains will be needed to better constrain their origin(s).

## ACKNOWLEDGEMENTS

The authors thank two anonymous reviewers for their helpful comments. This work was supported by NASA's Cosmochemistry program (L.R.N.). A.N. acknowledges support from the Carnegie Institution of Washington. The authors acknowledge the pioneering and inspirational work of Dr. Ernst Zinner in presolar grain research. His scientific fervor, generosity, and mentorship have left a lasting imprint on this multi-disciplinary field.

## APPENDIX A. SUPPLEMENTARY MATERIAL

Supplementary data associated with this article can be found, in the online version, at http://dx.doi.org/10.1016/j.gca.2017.02.026.

## REFERENCES

Abia C. and Isern J. (2000) The chemical composition of carbon stars II: the J-type stars. *Astrophys. J.* **536**, 438–449.

Alexander C. M. O'D. (1993) Presolar SiC in chondrites: how variable and how many sources? *Geochim. Cosmochim. Acta* **57**, 2869–2888.

Alexander C. M. O'D. and Nittler L. R. (1999) The galactic evolution of Si, Ti and O isotopic ratios. *Astrophys. J.* **519**, 222–235.

Amari S., Anders E., Virag A. and Zinner E. (1990) Interstellar graphite in meteorites. *Nature* **345**, 238–240.

Amari S., Hoppe P., Zinner E. and Lewis R. S. (1992) Interstellar SiC with unusual isotopic compositions: grains from a supernova? *Astrophys. J.* **394**, L43–L46.

Amari S., Lewis R. S. and Anders E. (1994) Interstellar grains in meteorites: I. Isolation of SiC, graphite, and diamond; size distributions of SiC and graphite. *Geochim. Cosmochim. Acta* **58**, 459–470.

Amari S., Hoppe P., Zinner E. and Lewis R. S. (1995) Trace-element concentrations in single circumstellar silicon carbide grains from the Murchison meteorite. *Meteoritics* **30**, 679–693.

Amari S., Zinner E. and Lewis R. S. (1999) A singular presolar SiC grain with extreme $^{29}$Si and $^{30}$Si excesses. *Astrophys. J.* **517**, L59–L62.

Amari S., Gao X., Nittler L. R., Zinner E., José J., Hernanz M. and Lewis R. S. (2001a) Presolar grains from novae. *Astrophys. J.* **551**, 1065–1072.

Amari S., Nittler L. R., Zinner E., Gallino R., Lugaro M. and Lewis R. S. (2001b) Presolar SiC grains of type Y: origin from low-metallicity AGB stars. *Astrophys. J.* **546**, 248–266.

Amari S., Nittler L. R., Zinner E., Lodders K. and Lewis R. S. (2001c) Presolar SiC grains of type A and B: their isotopic compositions and stellar origins. *Astrophys. J.* **559**, 463–483.

Asplund, M. (1999). Sakurai's object - stellar evolution in real time. In: Le Bertre, T., Lèbre, A., and Waelkens, C. (Eds.), *I.A.U. Symposium 191*.

Asplund M., Lambert D. L., Kipper T., Pollacco D. and Shetrone M. D. (1999) The rapid evolution of the born-again giant Sakurai's object. *Astron. Astrophys.* **343**, 507–518.

Asplund M., Grevesse N., Sauval A. J. and Scott P. (2009) The chemical composition of the Sun. *Ann. Rev. Astron. Astrophys.* **47**, 481–522.

Bernatowicz T., Fraundorf G., Tang M., Anders E., Wopenka B., Zinner E. and Fraundorf P. (1987) Evidence for interstellar SiC in the Murray carbonaceous meteorite. *Nature* **330**, 728–730.

Bernatowicz T. J., Messenger S., Pravdivtseva O., Swan P. and Walker R. M. (2003) Pristine presolar silicon carbide. *Geochim. Cosmochim. Acta* **67**, 4679–4691.

Besmehn A. and Hoppe P. (2003) A NanoSIMS study of Si- and Ca-Ti-isotopic compositions of presolar silicon carbide grains from supernovae. *Geochim. Cosmochim. Acta* **67**, 4693–4703.

Busso M., Gallino R. and Wasserburg G. J. (1999) Nucleosynthesis in asymptotic giant branch stars: relevance for Galactic enrichment and solar system formation. *Ann. Rev. Astron. Astrophys.* **37**, 239–309.

Clayton D. D. (2003) Presolar galactic merger spawned the SiC grain mainstream. *Astrophys. J.* **598**, 313–324.

Cristallo S., Piersanti L., Straniero O., Gallino R., Domínguez I., Abia C., Di Rico G., Quintini M. and Bisterzo S. (2011) Evolution, nucleosynthesis, and yields of low-mass asymptotic giant branch stars at different metallicities. II. The FRUITY database. *ApJS* **197**, 17–37.

Floss C., Stadermann F. J., Kearsley A. T., Burchell M. J. and Ong W. J. (2013) The abundance of presolar grains in comet 81P/Wild 2. *Astrophys. J.* **763**, 140–150.

Fujiya W., Hoppe P., Zinner E., Pignatari M. and Herwig F. (2013) Evidence for radiogenic sulfur-32 in type AB presolar silicon carbide grains? *Astrophys. J. Lett.* **776**, L29–L34.

Gallino R., Arlandini C., Busso M., Lugaro M., Travaglio C., Straniero O., Chieffi A. and Limongi M. (1998) Evolution and nucleosynthesis in low-mass asymptotic giant branch stars. II. Neutron capture and the s-process. *Astrophys. J.* **497**, 388–403.

Gallino R., Raiteri C. M., Busso M. and Matteucci F. (1994) The puzzle of silicon, titanium and magnesium anomalies in meteoritic silicon carbide grains. *Astrophys. J.* **430**, 858–869.

Gallino R., Busso M. and Lugaro M. (1997) Neutron capture nucleosynthesis in AGB stars. In *Astrophysical Implications of the Laboratory Study of Presolar Materials* (eds. T. J. Bernatowicz and E. Zinner). AIP, New York.

Gyngard F., Amari S., Jadhav M., Marhas K., Zinner E. and Lewis R. S. (2006) Titanium isotopic ratios in KJG presolar SiC grains from Murchison. *Meteorit. Planet. Sci.* **41**, A5334.

Hedrosa R. P., Abia C., Busso M., Cristallo S., Domínguez I., Palmerini S., Plez B. and Straniero O. (2013) Nitrogen isotopes in asymptotic giant branch carbon stars and presolar SiC grains: a challenge for stellar nucleosynthesis. *Astrophys. J. Lett.* **768**, L11.

Herwig F. (2001) The evolutionary timescale of Sakurai's Object: a test of convection theory? *Astrophys. J.* **554**, L71–L74.

Herwig F., Pignatari M., Woodward P. R., Porter D. H., Rockefeller G., Fryer C. L., Bennett M. and Hirschi R. (2011) Convective-reactive proton-$^{12}$C combustion in Sakurai's object (V4334 Sagittarii) and implications for the evolution and yields from the first generations of stars. *Astrophys. J.* **727**, 89.

Hoppe P., Amari S., Zinner E., Ireland T. and Lewis R. S. (1994) Carbon, nitrogen, magnesium, silicon and titanium isotopic compositions of single interstellar silicon carbide grains from the Murchison carbonaceous chondrite. *Astrophys. J.* **430**, 870–890.

Hoppe P., Annen P., Strebel R., Eberhardt P., Gallino R., Lugaro M., Amari S. and Lewis R. S. (1997) Meteoritic silicon carbide grains with unusual Si-isotopic compositions: evidence for an origin in low-mass, low-metallicity asymptotic giant branch stars. *Astrophys. J.* **487**, L101–L104.

Hoppe P. and Besmehn A. (2002) Evidence for extinct vanadium-49 in presolar silicon carbide grains from supernovae. *Astrophys. J.* **576**, L69–L72.

Hoppe P., Leitner J., Groner E., Marhas K. K., Meyer B. S. and Amari S. (2010) NanoSIMS studies of small presolar SiC grains: new insights into supernova nucleosynthesis, chemistry, and dust formation. *Astrophys. J.* **719**, 1370–1384.

Hoppe P., Fujiya W. and Zinner E. (2012) Sulfur molecule chemistry in supernova ejecta recorded by silicon carbide stardust. *Astrophys. J. Lett.* **745**, L26–L30.

Hoppe P., Strebel R., Eberhardt P., Amari S. and Lewis R. S. (1996) Type II supernova matter in a silicon carbide grain from the Murchison meteorite. *Science* **272**, 1314–1316.

Hoppe P. and Ott U. (1997) Mainstream silicon carbide grains from meteorites. In *Astrophysical Implications of the Laboratory Study of Presolar Materials* (eds. T. J. Bernatowicz and E. Zinner). AIP, New York.

Hoppe P., Strebel R., Eberhardt P., Amari S. and Lewis R. S. (2000) Isotopic properties of silicon carbide X grains from the Murchison meteorite in the size range 0.5–1.5 μm. *Meteorit. Planet. Sci.* **35**, 1157–1176.

Huss G. R., Hutcheon I. D. and Wasserburg G. J. (1997) Isotopic systematics of presolar silicon carbide from the Orgueil (CI) carbonaceous chondrite: implications for solar system formation and stellar nucleosynthesis. *Geochim. Cosmochim. Acta* **61**, 5117–5148.

Huss G. R. and Smith J. B. (2007) Titanium isotopic compositions of well-characterized silicon carbide grains from Orgueil (CI): implications for s-process nucleosynthesis. *Meteorit. Planet. Sci.* **42**, 1055–1075.

Hutcheon I. D., Huss G. R., Fahey A. J. and Wasserburg G. J. (1994) Extreme $^{26}$Mg and $^{17}$O enrichments in an Orgueil corundum: identification of a presolar oxide grain. *Astrophys. J.* **425**, L97–L100.

Hynes, K. M. and Gyngard, F. (2009). The Presolar Grain Database: http://presolar.wustl.edu/~pgd. *Lunar & Planetary Science* **XL**, Abstract #1198.

Ireland T. R., Zinner E. K. and Amari S. (1991) Isotopically anomalous Ti in presolar SiC from the Murchison meteorite. *Astrophys. J.* **376**, L53–L56.

Jadhav M., Amari S., Marhas K. K., Zinner E., Maruoka T. and Gallino R. (2008) New stellar sources for high-density, presolar graphite grains. *Astrophys. J.* **682**, 1479–1485.

Jadhav M., Pignatari M., Herwig F., Zinner E., Gallino R. and Huss G. R. (2013) Relics of ancient post-AGB stars in a primitive meteorite. *Astrophys. J. Lett.* **777**, L27.

Kipper T. and Klochkova V. G. (1997) The chemical composition of Sakurai's object. *Astron. Astrophys.* **324**, L65–L68.

Lambert D. L., Gustafsson B., Eriksson K. and Hinkle K. H. (1986) The chemical composition of carbon stars. I. Carbon, nitrogen, and oxygen in 30 cool carbon stars in the galactic disk. *Astrophys. J. Suppl.* **62**, 373–425.

Lewis R. S., Tang M., Wacker J. F., Anders E. and Steel E. (1987) Interstellar diamonds in meteorites. *Nature* **326**, 160–162.

Lewis K. M., Lugaro M., Gibson B. K. and Pilkington K. (2013) Decoding the message from meteoritic stardust silicon carbide grains. *Astrophys. J. Lett.* **768**, L19.

Lin Y., Gyngard F. and Zinner E. (2010) Isotopic analysis of supernova SiC and $Si_3N_4$ grains from the Qingzhen (EH3) chondrite. *Astrophys. J.* **709**, 1157–1173.

Liu N., Nittler L. R., Alexander C. M. O'D., Wang J., Pignatari M., José J. and Nguyen A. (2016) Stellar origins of extremely $^{13}C$- and $^{15}N$-enriched presolar SiC grains: novae or supernovae? *Astrophys J* **820**, 140.

Lodders K. and Fegley, Jr., B. (1997) Condensation chemistry of carbon stars. In *Astrophysical Implications of the Laboratory Study of Presolar Materials* (eds. T. J. Bernatowicz and E. Zinner). AIP, New York.

Lugaro M., Zinner E., Gallino R. and Amari S. (1999) Si isotopic ratios in mainstream presolar SiC grains revisited. *Astrophys. J.* **527**, 369–394.

Lugaro M., Davis A. M., Gallino R., Pellin M. J., Straniero O. and Käppeler F. (2003) Isotopic compositions of strontium, zirconium, molybdenum, and barium in single presolar SiC grains and asymptotic giant branch stars. *Astrophys. J.* **593**, 486–508.

Messenger S., Keller L. P., Stadermann F. J., Walker R. M. and Zinner E. (2003) Samples of stars beyond the solar system: silicate grains in interplanetary dust. *Science* **300**, 105–108.

Meyer B. S., Krishnan T. D. and Clayton D. D. (1996) $^{48}Ca$ production in matter expanding from high temperature and density. *Astrophys. J.* **462**, 825–838.

Nguyen A. N. and Zinner E. (2004) Discovery of ancient silicate stardust in a meteorite. *Science* **303**, 1496–1499.

Nittler L. R., Alexander C. M. O'D., Gao X., Walker R. M. and Zinner E. K. (1994) Interstellar oxide grains from the Tieschitz ordinary chondrite. *Nature* **370**, 443–446.

Nittler L. R., Amari S., Zinner E., Woosley S. E. and Lewis R. S. (1996) Extinct $^{44}Ti$ in presolar graphite and SiC: proof of a supernova origin. *Astrophys. J.* **462**, L31–L34.

Nittler L. R., Alexander C. M. O'D., Gao X., Walker R. M. and Zinner E. (1997) Stellar sapphires: the properties and origins of presolar $Al_2O_3$ in meteorites. *Astrophys. J.* **483**, 475–495.

Nittler L. R. and Alexander C. M. O'D. (2003) Automated isotopic measurements of micron-sized dust: application to meteoritic presolar silicon carbide. *Geochim. Cosmochim. Acta* **67**, 4961–4980.

Nittler L. R. (2005) Constraints on heterogeneous galactic chemical evolution from meteoritic stardust. *Astrophys. J.* **618**, 281–296.

Nittler L. R. and Hoppe P. (2005) Are presolar silicon carbide grains from novae actually from supernovae? *Astrophys. J.* **631**, L89–L92.

Nittler L. R., Hoppe P., Alexander C. M. O'D., Amari S., Eberhardt P., Gao X., Lewis R. S., Strebel R., Walker R. M. and Zinner E. (1995) Silicon nitride from supernovae. *Astrophys. J.* **453**, L25–L28.

Nittler L. R., Liu N., Alexander C. M. O'D. and Wang J. (2016) Explosive H-burning and neutron capture isotopic signatures in $^{13}C$- and $^{15}N$-rich presolar SiC grains. *Meteorit. Planet. Sci.* **51**, A6204.

Nollett K. M., Busso M. and Wasserburg G. J. (2003) Cool bottom processes on the thermally pulsing asymptotic giant branch and the isotopic composition of circumstellar dust grains. *Astrophys. J.* **582**, 1036–1058.

Ohnaka K. and Tsuji T. (1999) Quantitative analysis of carbon isotopic ratios in carbon stars. III. 26 J-type carbon stars including 5 silicate carbon stars. *Astron. Astrophys.* **345**, 233–243.

Palmerini S., La Cognata M., Cristallo S. and Busso M. (2011) Deep mixing in evolved stars. I. The effect of reaction rate revisions from C to Al. *Astrophys. J.* **729**, 3–24.

Savina, M. R., Pellin, M. J., Davis, A. M., Lewis, R. S., and Amari, S. (2007). p-process signature in a unique presolar silicon carbide grain. *Lunar & Planetary Science* XXXVIII, Abstract #2231.

Savina, M. R., Tripa, C. E., Pellin, M. J., Davis, A. M., Clayton, R. N., Lewis, R. S., and Amari, S. (2003). Isotopic composition of molybdenum and barium in single presolar silicon carbide grains of type A+B. *Lunar Planet. Sci.* XXXIV, Abstract #2079.

Stadermann F. J., Croat T. K., Bernatowicz T. J., Amari S., Messenger S., Walker R. M. and Zinner E. (2005) Supernova graphite in the NanoSIMS: carbon, oxygen and titanium isotopic compositions of a spherule and its TiC sub-components. *Geochim. Cosmochim. Acta* **69**, 177–188.

Timmes F. X. and Clayton D. D. (1996) Galactic evolution of silicon isotopes: application to presolar SiC grains from meteorites. *Astrophys. J.* **472**, 723–741.

Timmes F. X., Woosley S. E. and Weaver T. A. (1995) Galactic chemical evolution: hydrogen through zinc. *Astrophys. J. Suppl.* **98**, 617–658.

Tizard J. M., Lyon I. C. and Henkel T. (2005) The gentle separation of interstellar SiC grains from meteorites. *Meteorit. Planet. Sci.* **40**, 335–342.

Utsumi K. (1985) Abundance analysis of cool carbon stars. In *Cool Stars with Excesses of Heavy Elements* (eds. M. Jaschek and P. C. Keenan). Springer, Netherlands, Dordrecht.

Virag A., Wopenka B., Amari S., Zinner E., Anders E. and Lewis R. S. (1992) Isotopic, optical, and trace element properties of large single SiC grains from the Murchison meteorite. *Geochim. Cosmochim. Acta* **56**, 1715–1733.

Woosley S. E. (1997) Neutron-rich nucleosynthesis in carbon deflagration supernovae. *Astrophys. J.* **476**, 801–810.

Xu Y., Zinner E., Gallino R., Heger A., Pignatari M. and Lin Y. (2015) Sulfur isotopic compositions of submicrometer SiC grains from the murchison meteorite. *Astrophys. J.* **799**, 156.

Zinner E. (2014) Presolar grains. In *Treatise on Geochemistry* (eds. H. D. Holland and K. K. Turekian), second ed. Elsevier, Oxford.

Zinner E., Amari S., Guinness R., Jennings C., Mertz A. F., Nguyen A. N., Gallino R., Hoppe P., Lugaro M., Nittler L. R.

and Lewis R. S. () NanoSIMS isotopic analysis of small presolar grains: search for $Si_3N_4$ grains from AGB stars and Al and Ti isotopic compositions of rare presolar SiC grains. *Geochim. Cosmochim. Acta* **71**, 4786–4813.

Zinner E., Jadhav M., Gyngard F. and Nittler L. R. (2011) Bonanza, a huge presolar SiC grain of type X. *Lunar Planet. Sci.* **42**. Abstract #1070.

Zinner E., Nittler L. R., Gallino R., Karakas A. I., Lugaro M., Straniero O. and Lattanzio J. C. (2006) Silicon and carbon isotopic ratios in AGB stars: SiC grain data, models, and the Galactic evolution of the Si isotopes. *Astrophys. J.* **650**, 350–373.

*Associate editor:* Anders Meibom